The influence of land use and land cover change on landslide susceptibility: A case study in Zhushan Town, Xuanen County (Hubei, China)

Lixia Chen[1*], Zizheng Guo[2], Kunlong Yin[2], Dhruba Pikha Shrestha[3], Shikuan Jin[4]

[1]Institute of Geophysics and Geomatics, China University of Geosciences , wuhan, 430074, China

[2]Engineering Faculty, China University of Geosciences , wuhan, 430074, China

[3]Department of Earth Systems Analysis, Faculty of Geo-Information Science and Earth Observation (ITC), University of Twente, Enschede, 7500 AE, The Netherlands

[4]State Key Laboratory of Information Engineering in Surveying, Mapping and Remote Sensing, Wuhan University, wuhan, 430079, China

[*]*Correspondence to:* Lixia Chen (**lixiachen@cug.edu.cn**) *Co-first author:* Zizheng Guo (**cuggzz@cug.edu.cn**)

Abstract: Land use and land cover change can have effect on the land by increasing/decreasing landslide susceptibility (LS) in the mountainous areas. In the southwestern hilly and mountainous part of China, land use and land cover change (LUCC) has been taking place in the recent past due to infrastructure development and increase in economic activities. These development activities can also bring negative effects: the sloping area may become susceptible to landslides due to undercutting of slopes. The study aims at evaluating the influence of land use and land cover change on landslide susceptibility at regional scale, based on the application of Geographic Information System (GIS) and Remote Sensing (RS) technologies. The Zhushan Town, Xuanen County in the southwest of China was taken as the study area and the spatial distribution of landslides was determined from visual interpretation of aerial photographs and remote sensing images, as well as field survey. Two types of land use/land cover (LUC) maps, with a time interval covering 21 years (1992-2013), were prepared: the first was obtained through the neural net classification of images acquired in 1992, the second through the object-oriented classification of images in 2002 and 2013. Landslide susceptible areas were analyzed using logistic regression models. In this process, six landslide influencing factors were chosen as the landslide susceptibility indices. Moreover, we applied a hydrologic analysis method achieving slope unit (SU) delineation to optimize the partitioning of the terrain. The results indicate that the LUCC in the region was mainly the transformation from the grassland and arable land to the forest land and the human engineering activities land (HEAL). The areas of these two kind of LUC increased by 34.3% and 1.9%, respectively. The comparison of landslide susceptibility maps in various periods revealed that human engineering activities was the most important factor to increase LS in this region. Such results underline that a more reasonable land use planning in the urbanization process is necessary.

Keywords: land use and land cover change; landslide susceptibility; Geographic Information System; neural network

classification; object-oriented image analysis; slope unit; logistic regression model

1 Introduction

Landslide constitutes one of the most hazardous geomorphic processes in mountain areas (Karsli et al., 2009), which can result in serious injuries, human casualties and cause environmental and economic damages on a yearly basis (Fell et al., 2008; García-Ruiz et al., 2010). It is therefore necessary to take landslide hazard into account for public safety and realization of safe engineering projects (Fell et al., 2008; Gioia et al., 2015). As landslide is the results of the complex spatial-temporal interaction of many factors (Pisano et al., 2017), numerous environmental factors (e.g., slope angle, slope morphology, topography, lithology and hydrology) have been defined as the main criteria in the literatures (Guzzetti et al., 2006a; Nandi and Shakoor, 2009; Pourghasemi and Rossi, 2017). Moreover, some studies have indicated that the human-induced land use and land cover change (LUCC) contributes significantly to the initiation and reactivation of landslides (Guillard and Zêzere, 2012; Galve et al., 2015; Meneses, et al., 2019), especially in populated regions, where landslides represent a major risk to human settlements, infrastructure and population (Pinyol et al., 2012; Abancó and Hürlimann, 2014). So this factor should not be ignored in the process of landslide risk reduction, particularly against the background of adaptation to sustainable natural hazard risk management (Promper et al., 2015; Wang et al., 2018).

LUCC often implies both modifications in the natural and social systems (Promper et al., 2015; Lopez-Saez et al., 2016), in particular to changes in vegetation cover (Tasser et al., 2003; Schmaltz et al., 2017), under cutting of slopes (Scalenghe and Marsan, 2009), surface sealing or changes of drainage system (Ghestem et al., 2011, 2014), all of which potentially influence landslide hazard processes. For example, the phenomenon that mountainous areas with forest cover typically appear to be less susceptible to shallow landslides than unforested mountain slopes as described in many studies such as Curden and Miller (2001), Beguería (2006) and Galve et al. (2015). Similarly, deforestation followed by engineering activities e.g. road and/or railway construction, under cutting of slopes, development of settlement areas, buildings, etc. in steep mountainous areas increases the vulnerability to landslide hazard (Glade, 2003; Bruschi et al., 2013). All these modifications generally lead to an increase in the rate of landslide occurrences, which are strongly conditioned by land use and land cover (LUC) and hillslope morphology (Cervi et al., 2010; Piacentini et al., 2012; Reichenbach et al., 2014). These are the reasons why land use planning should be closely linked with landslide risk assessment (Glade, 2003; van Westen et al., 2006; Fell et al., 2008). For single slopes and small-scale areas, the impact of the plant root system or the spatial distribution of LUC on landslides have been evaluated by various methods, including digital photogrammetric techniques (Karsli et al., 2009), microstructure analysis (Ghestem et al., 2011), laboratory shear tests (Ghestem et al., 2011), numerical modelling approaches (Mao et al., 2014) and so on. From the perspective of the regional scale, within an effective hazard mitigation planning, the landslide susceptibility (LS) is usually considered as the initial work (Chen et al., 2016; Zhou et al., 2018) which can be used to reflect the degree to which a terrain unit can be affected by future slope movements (van Westen et al., 2008; Lombardo and Mai, 2018). The importance of the influence of LUCC in landslide susceptibility analysis in regional scale, has been noted by several authors (Reichenbach et al., 2014; Pisano et al., 2017; Meneses et al., 2019).

During the past decades, various techniques incorporating geographical information system (GIS) along with remote sensing (RS) technologies have been widely used to map slope stability e.g. quantifying landslide hazards in relation to LUCC (Meneses et al., 2019), use of spatial statistical analysis (Kayastha, 2015), aerial photogrammetry (Karsli et al., 2009; Bruschi et al., 2013), using spaceborne optical sensors data (Taubenböck et al., 2011; Li et al., 2019) and time-lapse photography for soil aggregate stability (Ymeti et al., 2017). For such studies, in general, the selection of meaningful mapping units is a basis step because it is of great importance for susceptibility zonation . A mapping unit refers to a portion of land surface with analogous geologic and/or geomorphic properties (Guzzetti et al., 2006b), which can broadly be summarized into four categories: grid cells, slope units (SU), terrain units (TU) and unique condition units, of which grid cells and SU are the most widely used (Van Den Eeckhaut et al., 2009; Rotigliano et al., 2012; Chen et al., 2016). Each category of mapping units presents advantages and disadvantages. Despite the long-term efforts by researchers, the adoption of the best mapping unit still remains a conceptual problem and an operational challenge (Guzzetti et al., 2000; Alvioli et al., 2016). In addition to the extensive discussions about this subject (Guzzetti et al., 1999; Aleotti and Chowdhury, 1999; Brenning, 2005), several authors have provided examples where different mapping units were tested for the same area (Van Den Eeckhaut et al., 2009; Rotigliano et al., 2012). We can see that mostly the current trend of using grid cells is unjustified (Schlögel et al., 2018), especially considering single cell values are less representative for phenomena involving portion or whole slopes (Camilo et al., 2017); rather, a SU considers the totality of the slopes where the landslides occurred and can forecast the spatial locations of future independent landslides. As a consequence, the SU can be the correct spatial domain to operate upon.

In Zhushan Town, land use and land cover change has been taking place in the recent past due to infrastructure development and increase in economic activities. These processes have also caused damage to the geological environment, mainly in three aspects: (i) Constructions of infrastructures and residential buildings built on hillslopes, which resulted in steep slopes by under cutting and backfilling; (ii) Construction of mines, which led to the destruction of cultivated and forest lands; (iii) As the most important water conservancy and hydropower engineering facility in the county, the Shuanglonghu Reservoir (SLHR) was built in 1992, which is located near the urban area. The change of seepage conditions caused by the dynamic change of the reservoir water level has a great impact on the stability of the slopes on both sides. The aim of our work is thus to explore the relationship between LUCC and the regional landslide susceptibility. It is of utmost important to know the main land cover land use processes, which is responsible for landslide susceptibility so that preventive measures can be implement from the beginning. Landslide inventory was carried out and causal factors were determined. Different LUC maps for three periods with a time interval covering 21 years (1992-2013) were prepared using remote sensing techniques. Finally, landslide susceptibility assessment was carried out in GIS environment and subsequently compared to evaluate the impact of the LUCC during this period.

2 Materials

2.1 Study area

2.1.1 General description

Xuanen County in southwest of Hubei Province (China) was selected as the study area, which is about 45 km away from the Enshi city (Fig. 1). The study area lies within longitude 109°11′-109°55′ east and latitude 29°33′-30°12′ north, with surface area covering 2740 km^2, among which, Zhushan Town is located in the northwestern Xuanen County with a surface area covering approximately 49 km^2. The region belongs to the extension of Wuling and Qiyue Mountains and surrounded by middle and low mountains, with an elevation ranging from 350 m to 2015 m above sea level (ASL). The elevation range in most areas is 350 m - 2015 m ASL, characterized by high northwest and low southeast in the terrain. The region is located at the end of the syncline core, which spreads along the NE-SW direction. Influenced by this, the joints of NE and NW direction in the region are developed, destroying the integrity of the rock mass to some extent.

The climate of the study area is subtropical monsoon, and it can vary locally due to elevation differences. In the area with the elevation below 800 m ASL, the average annual rainfall is about 1500 mm, which gradually increases with increase in elevation. When the elevation is above 1200 m ASL, the average annual rainfall exceeds 1800 mm. From the perspective of the strata, the sedimentary rocks from the Cambrian to the Cretaceous and the loose Quaternary deposits compose the strata in Xuanen County, of which the main outcropping strata consist of the Badong Formation of middle Triassic (T_2b) and the Quaternary deposits. The Gongshui River is the main stream in the area, with the Shuanglong Lake Reservoir built at the upriver. Under the normal working conditions, the water level is about 490 m ASL. In the case of heavy rain or reservoir flood releasing, the water level usually increases by 1~2 m.

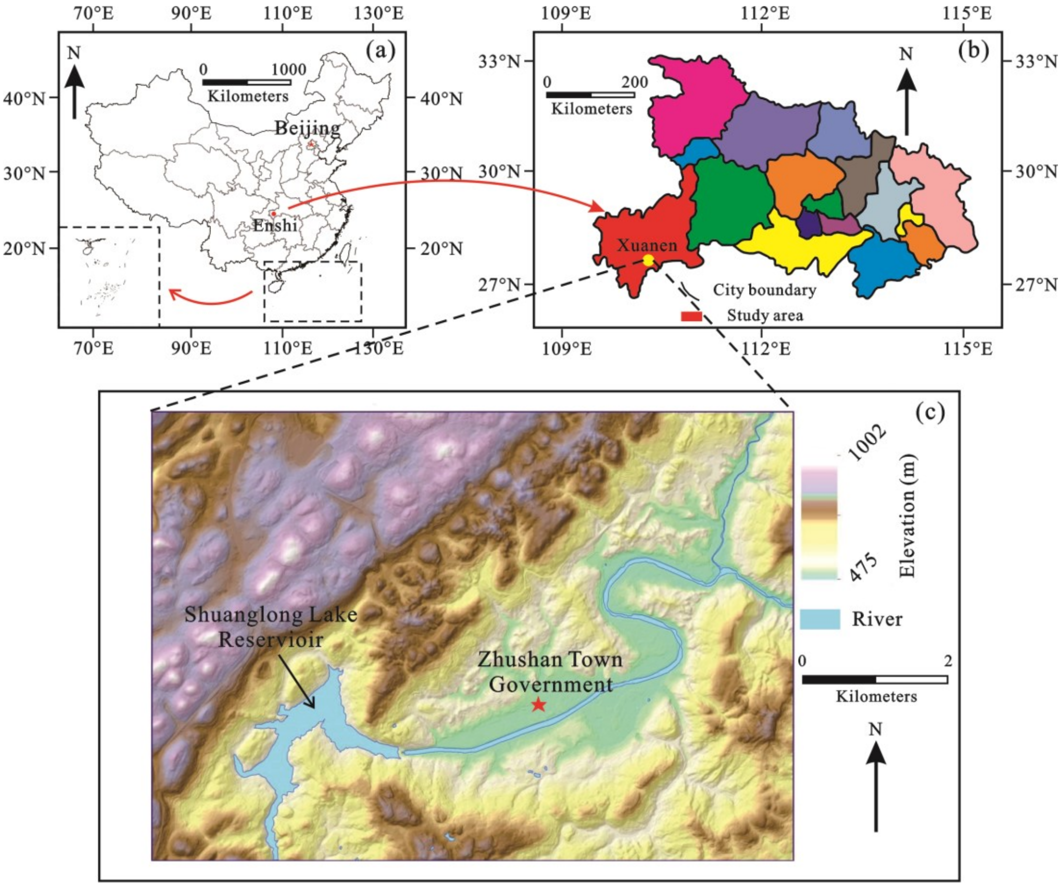

Fig. 1 The location of the study area: (a) The location of Hubei Province in China. (b) The location of Xuanen County in Hubei Province. (c) The digital elevation model (DEM) showing the basic terrain conditions

2.1.2 Urbanization and human engineering activities

Before the 1980s, the settlements in Xuanen County were small, with poor infrastructures and limited functions. With the rapid development of the economy in the recent past, expansion of settlement areas took place on a yearly basis, reflected by the construction of highways, in addition to the nearly doubled number of industrial and civil buildings. By early 1990s, surface area of Zhushan Town had increased significantly, of which the urban area mainly concentrated in the north side of the Gongshui River valley plain. Meanwhile, most areas surrounding the urban area were bare land or cultivated land or deforested. With the constructions of infrastructures, especially along the No. 209 national road, the traffic condition has been further improved and the tertiary industry (construction industry, tourism, etc.) has gradually become the pillar industry of the area. At present, Zhushan Town has become the political and economic center of the entire county, and the urban area has expanded on the both sides of the entire river valley plain, as well as the steep mountain areas outside the valley. The urban area has grown from the initial 0.5 km^2 to nearly 7 km^2 (an increase of 14 times) with current population of 75000 residents, making it as one of the most densely populated towns in the county.

Since the main terrain condition in the study area is hilly and mountainous, the available land resources become limited. In the process of urbanization in recent decades, many engineering activities carried out in the area have transformed the original topography of the area by various levels. Although the urbanization process has improved the economic level of the study area, the LUCC caused by construction activities has also become one of the main factors influencing slope deformation and failure.

2.2 Data sources

The data used in the study mainly includes: (i) the topographic map, and (ii) the geological map for various influencing factor maps; (iii) detailed landslide reports, (iv) aerial photographs and (v) RS images for landslide inventory map and LUC map. Details on the data as well as details on spatial resolution and acquisition dates of satellite data are shown in Table 1.

Table 1 The sources and characteristics of the data used in the paper

No.	Data	Scale	Resolution	Source	Purpose
1	Topographic map	1:50000	10 m	China Geological Survey (Wuhan Center)	Landslide influencing factor maps
2	Geological map	1:100000	20 m		
3	Landslide reports	/	/	China Geological Survey (Wuhan Center)	Landslide inventory map
4	Aerial photographs	/	2048*1536 dpi	DJI drone	
5	Google Earth images	/	30 m	Google (https://google-earth.en.softonic.com/)	
6	RS images	/	30 m	Landsat4-5TM (28 August 1992)	LUC maps
7	RS images	/	2 m	Superview-1 (25 September 2002 And 20 September 2013)	

3 Methodology

3.1 Land use and land cover mapping

Satellite remote sensing can be used to obtain sufficient data for extracting land use and land cover information. The key step in this process is the RS images classification (Shrestha et al., 2019). For cases of different years, it seems to be more reasonable to use the same analysis method, especially considering the end result, which is LUC maps. Moreover, in order to make the results more accurate, the RS data quality should also be taken into account, which is mainly associated with the resolution of satellite images. In the 1990s highest resolution of multispectral images was 30 m (Landsat TM), which allows optimal pixel based classification. With the development of high-resolution RS images, object-oriented techniques, using polygon entity as the basic unit, provide a widely-used method for information processing (Blaschke, 2010; Bayramov et al., 2016; Ymeti et al., 2017). Hence, for the present study both pixel-based as well as the object-oriented methods were chosen for the classifications of images in 1992, 2002 and 2013.

Three sets of RS images were prepared to obtain the LUC maps of different years: Landsat4-5TM images from 1992, superview-1 images from 2002 and superview-1 images from 2013. For the Landsat4-5TM images, normalized difference vegetation index (NDVI) (Huang et al., 2018) and normalized difference water index (NDWI) (Li et al., 2019) were obtained using ENVI software (http://www.harrisgeospatial.com/docs/using_envi_Home.html). Then the first five bands (wavelength ranges of 0.45~0.52μm, 0.52~0.60μm, 0.63~0.69μm, 0.76~0.90μm and 1.55~1.75μm, respectively) of images as well as the NDVI and NDWI were selected together for neural net classification, of which the training samples were the regions of interest determined by visual interpretation. Logistic function was determined as the activation. The number of hidden layers was set to 1 and the training rate was set to 0.5. The termination condition was set to 10^{-4} and the number of training iterations was set to 500. For the superview-1 images, the multiscale segmentation was performed based on eCognition software (http://www.ecognition.com/). The parameters were set as: (i) scale parameter: 200, (ii) band weight: blue 1, Green 1 and red 1, (iii) shape: 0.6, and (iv) compactness: 0.4. Then, considering the average brightness, length-width-height ratio and shape index of the object as the features, nearest neighbor classification was carried out, where the way to obtain the ROI was similar with that in the ENVI.

3.1.1 Pixel-based analysis: neural network (NN) classification

NN classification aims at comparing pixels to one another and to those of known identity by using neural network algorithm, and then assigning groups of identical pixels found in remotely sensed data into classes that match the informational categories of user interest (Abdul-Qadir, 2014). Among numerous NN models developed for pattern recognition (Berberoglu et al., 2000; Aitkenhead et al., 2008), BP neural network (BPNN) is the most commonly used. The basic element of a BPNN is the processing node and the interconnections between each node have an associated weight (Lee et al., 2004). These nodes are organized into layers, and each layer is fully interconnected to the following layer in general.

Each BPNN consists of three or more interconnected layers: input layer (i.e., the first layer), output layer (i.e., the final processing layer) and hidden layer (between input layer and output layer). The number of hidden layers and nodes within each layer can be defined by the user.

In RS images, each pixel in the image has own specific LUC information. Although mostly it is impossible to state the clear LUC characteristics of all pixels, we can still determine the LUC properties of part of the pixels by statistics files, field work or known live photos. Then these pixels are considered as region of interest (ROI) and their LUC information are extracted directly from the image as the training dataset of the BPNN. This dataset is input into the nodes of the first layer and each processing node sums the values of its weighted inputs. The summed input signals are then transformed and passed to the nodes in the next layer in a feed-forward manner. After each training, the output results are compared with the actual LUC values, and the errors will be returned to the input layer for correction. Therefore, with the constant iteration of the training times, the final classification accuracy is gradually improved.

3.1.2 Object-oriented analysis: multiscale segmentation and nearest neighbor classification

The high resolution satellite imagery (HRSI) have higher spatial resolution and less spectrum number, so there are some "object with different spectra, different objects with same spectrum" phenomena (Zhang and Tang, 2019). In such images, pixels are smaller than the object so grouping of pixels is possible in order to obtain real-world homogeneous features (Blaschke, 2010; Ymeti et al., 2017). After the grouping, the smallest unit of the image in the classification process is not a pixel but the image object. It should be noted that spectral information, as well as the geometric and structural information should be all considered for subsequent analysis and processing.

Multiscale segmentation is a bottom-up image segmentation method based on two-two region merging techniques. It can perform multiple and continuous merging of pixels and ensure good homogeneity of all pixels in the same object of the image. There are three important parameters influencing the segmentation results: scale parameter, band weight and shape factor. The scale factor can determine the size of the object after the segmentation, as well as the final accuracy of the extracted information. The band weight can determine whether a specific band in the image is considered in the segmentation and the degree of the influence of this band. The shape factor can ensure the shape integrity of the object.

The eCognition software was selected as the tool for multiscale segmentation in this study, and the supervised classification based on nearest neighbor (NN) method was used. Similar with pixel-based analysis, this method allows to select region of interest (ROI) for taking training samples. In addition, it allows the description of samples in terms of shape and texture of the objects in the feature space. The classification of the test object is determined by the nearest neighbor.

The distance between the test and sample objects can be calculated as follows:

$$l = \sqrt{\sum_f \left(\frac{v_f^{(t)} - v_f^{(s)}}{\sigma_f}\right)^2} \tag{1}$$

where f is the order of the feature, $v_f^{(t)}$ is the feature values of the test object, $v_f^{(s)}$ is the feature values of the sample object, and σ_f is the standard deviation of the feature.

3.2 Logistic regression model

Numerous models have been developed to perform landslide susceptibility assessment, including heuristic, deterministic, statistical and machine learning models (Huang et al., 2017). Considering that the objective of our study is to observe the impact of LUCC in terms of their propensity to landslide initiation, a single mul-tivariate statistical classification model is suitable. Hence, we prepared the logistic regression model (LRM) to link the dependent variable expressing landslide probability with the independent variables (landslide influencing factors).

For LS assessment, LRM is a commonly used statistical technique that involves one or more independent explanatory variables to extract the empirical relationships from observations (Zhou et al., 2018).. In particular, through the addition of a suitable link function to the usual linear regression model, variables in the model may be either continuous or discrete, or any combination of both types and that they do not necessarily have normal distributions (Lee, 2005), which gives it an advantage over linear and log-linear regressions. Ozdemir et al (2013) and Lee (2005) have explained the detailed formula in the case of landslide susceptibility studies, which is denoted as follows:

$$Y = a + b_1X_1 + b_2X_2 + b_3X_3 + \cdots + b_mX_m \tag{2}$$

$$Y = \operatorname{logit}(P) = \ln\left(\frac{P}{1-P}\right) \tag{3}$$

$$p = \frac{e^Y}{1+e^Y} \tag{4}$$

where $X_1, X_2, \ldots, X_m$ are predictor variables and Y is a linear combination function of these variables that represent a linear relationship. If Y is used as a binary variable (0 or 1), then the value 0 or 1 represent the absence or presence of a landslide, respectively; The parameters a, $b_1, b_2, \ldots, b_m$ are the regression coefficients that must be estimated, among which is the intercept, and $b_1, b_2, \ldots, b_m$ are the coefficients that measure the contribution of the independent variables ($X_1, X_2, \ldots, X_m$) to the variations in Y; P is the probability that the target variable (Y) is 1; P/(1-P) is the so-called odd or frequency ratio. Through this process, the model can establish a function relationship between binary coded landslide events and the different factors used for landslide susceptibility assessment (Yalcin et al., 2011).

After the analysis of the relationship between the landslide and the predictor variables, the value of *P* can be considered as the landslide susceptibility index (*LSI*). In this study, the *LSI*s were divided into four classes e.g. very high, high, moderate and low, according to the reasonable thresholds of *LSI* determined by natural breaks method.

3.3 Receiver operating characteristic (ROC) curve

Although the statistical methods can evaluate the model performance effectively such as the frequency ratio (*FR*) index, they require reclassification of landslide susceptibility index (*LSI*) values, and the change of the different breakpoint values can result in various evaluation results. To remedy this, ROC curve is more commonly used to evaluate landslide susceptibility results due to the cutoff-independence of it.

Several indices (Fig. 2 (a)) are proposed to evaluate landslide-prone area classification in ROC method, including true positive (TP) rate, true negative (TN) rate, false positive (FP) rate, false negative (FN) rate, sensitivity and specificity. In simple terms, if a model predicts a positive value of a given variable (event forecast) and the value of the variable is actually positive (event), a TP prediction is obtained. On the opposite, if the value of the variable is actually negative (no event), a FP prediction is obtained (Corsini and Mulas, 2017). TN and FN predictions are classified following similar logical combinations. Based on this, the sensitivity (Sen), i.e., the percentage of correctly classified landslide cases, and the specificity (Spe) can be determined as follows:

$$\text{Sen} = \frac{\text{"Number of TP"}}{\text{"Number of TP"} + \text{"Number of FN"}} \tag{5}$$

$$\text{Spe} = \frac{\text{"Number of FP"}}{\text{"Number of FP"} + \text{"Number of TN"}} \tag{6}$$

The Sen is also considered as the true positive rate and the value (1 − Spe) is the rate of false positives (Melchiorre et al., 2008). Generally, High sensitivity indicates a high number of correct predictions whereas high specificity (low 1-Spe difference) indicates a low number of false positives (Mohammady et al., 2012). Hence, the Sen of the model is plotted against 1-Spe to obtain the ROC curve, and in most cases, the area under the curve (AUC) is utilized to evaluate the prediction ability of models, and the model is considered better if the value of AUC is larger (Fig. 2 (b)).

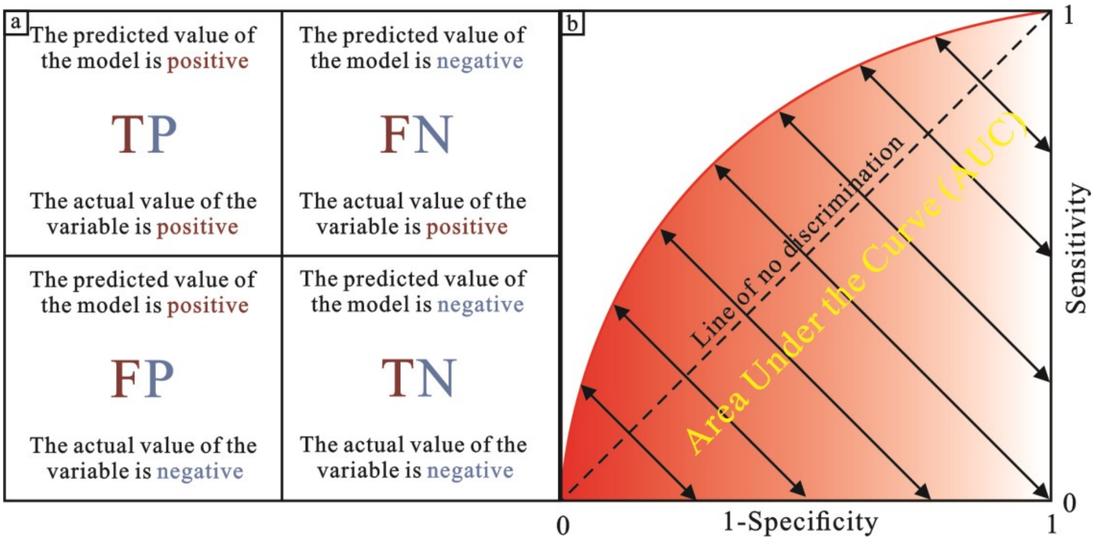

Fig. 2 (a) Some indices used to evaluate the landslide susceptible area classification in ROC method; (b) The example of ROC and AUC (source: Corsini and Mulas, 2017).

3.4 Slope unit

Slope unit (SU) is defined as one slope part, or the left/right part of a watershed, representing the region of space delimited between ridges and valleys under the constraint of homogeneous slope aspect and steepness distributions. It can avoid the shortcomings of low geomorphological representativeness of grid-based susceptibility mapping (Camilo et al., 2017). Hence, we adopted the SU as the mean to research landslide susceptibility in this study.

The SU can be drawn manually from topographic maps of adequate scale and quality or it can be delineated automatically using specialized software (Alvioli et al., 2016). According to the prevalent methods provided by the literatures (Xie et al., 2004; Reichenbach et al., 2014; Schlögel et al., 2018), the SUs of the study area were partitioned using ArcGIS-based hydrologic analysis method where SUs were the hydrological terrain subdivision bounded by drainage and divide lines. Slope units were generated as follows: (i) preparing the reverse DEM by subtracting the original DEM from the highest elevation of the study area; (ii) filling the original and the reverse DEM, respectively; (iii) extracting the surface water flow direction to distinguish areas with extremely rapid changes in surface morphology; (iv) establishing the stream link for obtaining the valley lines and ridge lines; (v) delineating the SUs based on the valley and ridge lines. One of the advantages of adopting slope units is that the computational burden is reduced due to lower number of units compared with the grid-based method (Camilo et al., 2017). Moreover, the SUs makes it possible to maximize the internal homogeneity and the external heterogeneity of the slope aspect (Mashimbye et al., 2014; Schlögel et al., 2018).

3.5 Landslide mapping and analysis

3.5.1 Landslide mapping

As the simplest form of landslide mapping, landslide inventory plays a very essential role in landslide susceptibility (Kayastha, 2015), especially in the initial phase of LS assessment because it provides the spatial distribution of locations of existing landslides (Tian et al., 2019). It can be done in a region using different techniques such as field survey, satellite image/air photo interpretation, and literature search for historical landslide records (Yalcin et al., 2011). The inventory was carried out from a combination of: (i) detailed reports from management institutes, (ii) visual interpretation of aerial photographs and remote sensing images, and (iii) field surveys carried out in the period from April to May 2013. To clarify the detailed landslide information, the landslide property database was also linked to the map, which includes the descriptions of some data that cannot be digitized, such as the amount, area and occurrence time of landslides and so on.

3.5.2 Factors influencing landslides

The spatial distribution of landslide hazards is the combined consequence of different factors, including not only internal geological backgrounds but also the external environmental settings. In this work, six influencing factors were determined first for LS analysis, i.e., slope, aspect, slope shape, lithology, distance to reservoir and LUC. These thematic data are collected from different sources. For example, elevation contour lines (1:50000 scale) and the geological map (1:100000 scale) were obtained from China Geological Survey, which were used for the extraction of topographic factors (i.e., slope, aspect and slope shape) and geological factors (i.e., lithology). The urban planning map, recording the detailed location of Shuanglonghu Reservoir, was collected from the government of Zhushan Town. The LUC maps were obtained from RS images.

The analysis for the relationship between landslide events and their triggering factors is a key step in landslide susceptibility assessment. In this study, this relationship was determined by the calculation of the ratio of the amount of units with landslide occurrence to the total amount of units in each class, namely the distribution curve of ratio. It should be noted that the original continuous variables (e.g., slope, aspect, etc.) cannot be input directly into the used model. in order to obtain a general knowledge about the effects of the variable on landslide occurrence, it is necessary to discretize these variables into subclasses according to the distribution curve of the frequency ratios (Huang et al., 2017). Moreover, after the selection and preliminary analysis of these factors, the conditional independence among them was tested. The results showed that all the variables were irrelevant due to the correlation coefficient of less than 0.2, so it is appropriate to take these factors into account for landslide susceptibility.

Topographic factors

From the elevation contour lines with intervals of 10 m, a digital elevation model (DEM) of the study area was prepared. Based on this DEM, topographic factors including slope, aspect and slope shape were obtained.

Slope angle (Fig. 3 (a)), defined as the steepness of a surface, is the major parameter of slope stability analysis which can helps us understanding the characteristics of a basin for runoff and erosion processes (Vasu and Lee, 2016). The slope angle of the study area varies greatly, with a range of 0°~73.6° and an average value of 21.3°. The continuous slope angles were divided into four categories: (i) flat to gentle slope (<15°); (ii) moderate slope (15-25°); (iii) steep slope (25-40°); (iv) very steep slope (>40°). From the perspective of spatial distribution, the flat to gentle slope angle mainly appears along the banks of the Gongshui River, while the surrounding mountains are steeper with the slope angle mainly varying from 20° to 45°. Based on the statistical results of LRM, the landslides mainly occurred in the moderate slope due to its regression coefficient values was the largest among all the categories. This is mainly because steep areas are generally the highest in elevation. Few human activities and disturbances on the geological conditions occur in such areas and therefore nearly no landslides have been detected in the inventory (Cervi et al., 2010; Zhou et al., 2018).

Aspect (Fig. 3 (b)) is also considered an important factor in landslide susceptibility assessment because many parameters in relation to aspect may affect the occurrence of landslides, such as exposure to sunlight, winds, rainfall (degree of saturation), and discontinuities (Yalcin et al., 2011). The aspect of this study was divided into eight categories. The statistical results revealed that the landslide is the easiest to occur on the aspect of 40-100° in all three years. Moreover, the categories of aspect, which have a positive effect in the occurrence of landslides are in the range of 100-120° and 260-300°, respectively.

Defined along the line of maximum slope, profile curvature (Fig. 3 (c)) affects the acceleration and deceleration of flow and, therefore, influences subsequent erosion and deposition (Regmi et al., 2010). However, the geological meaning of the profile curvature is not obvious. To remedy this, we classified the profile curvature map into three categories according to the values of the slope profile curvature: (i) convex; (ii) concave; (iii) straight (planar). These categories represent different slope shapes. In general, concave slopes are considered as potentially landslide-prone areas as they concentrate water at the lowest point, that can contribute to develop adverse hydrostatic pressure whereas convex slopes are more stable because they disperse the runoff more equally down the slope (Kayastha, 2015). This point can be confirmed by the model used in this study.

Lithology

The landslide event has a close relationship with the lithological characteristics of the land, because different rocks have different mechanical and hydrological properties (Van Westen et al., 2008). The lithology map (Fig. 3 (d)) of the study area was extracted from the geological map (1:100000 scale), which indicated that the main strata of Zhushan Town consist of Jianglingjiang Formation (T_1j) of lower Triassic (northwest of the urban area), Badong Formation (T_2b) of middle Triassic (most areas of the region) and the Quaternary deposits (banks of the Gongshui River). From the perspective of the material types, the T_2b is a kind of clastic rock composed of marine-terrigenous interdepositional mudstone, siltstone and marl (Deng et al., 2017), and the T_1j is a kind of carbonate rock composed of marine depositional dolomite, dolomitic limestones and microcrystalline limestone. Similarly, the Quaternary deposits also have several components, such as alluvium, proluvium and so on. Hence, according to the characteristics of engineering geology, these strata was differentiated into three lithological units: (i) the Quaternary deposits; (ii) layered clastic rock; (iii) layered carbonate rock with clastic rock. With the largest regression coefficient, the category of (ii) shows the strongest positive impact on the occurrence of landslides. More than 80% landslides developed in the stratum of layered clastic rock, although the amount of units of this category only accounts for 38.3% of the total units, which indicates that Badong Formation is a landslide-prone stratum.

Distance to reservoir

The large-scale engineering infrastructures can damage the initial geological conditions so that the slope stability is also influenced. In areas with abundant runoff, reservoir construction is the most common infrastructure development to make full use of water resources, but it also has been classified a significant factor inducing landslides (Iqbal et al., 2018), such as the Three Gorges Reservoir in China (Huang et al., 2017; Wang et al., 2018; Zhou et al., 2018). In order to see the effect of the Shuanglonghu Reservoir on landsliding, the distance to reservoir map (Fig. 3 (e)) was prepared, with a buffer distance of 200 m. Then, the study area was divided into three categories: (i) < 200 m; (ii) 200-400 m; (iii) > 400 m. We can see that although the area of the category of (i) and (ii) only accounts for about 5% of the whole region, the ratio of the units with the occurrences of landslide is larger than the category of (iii).

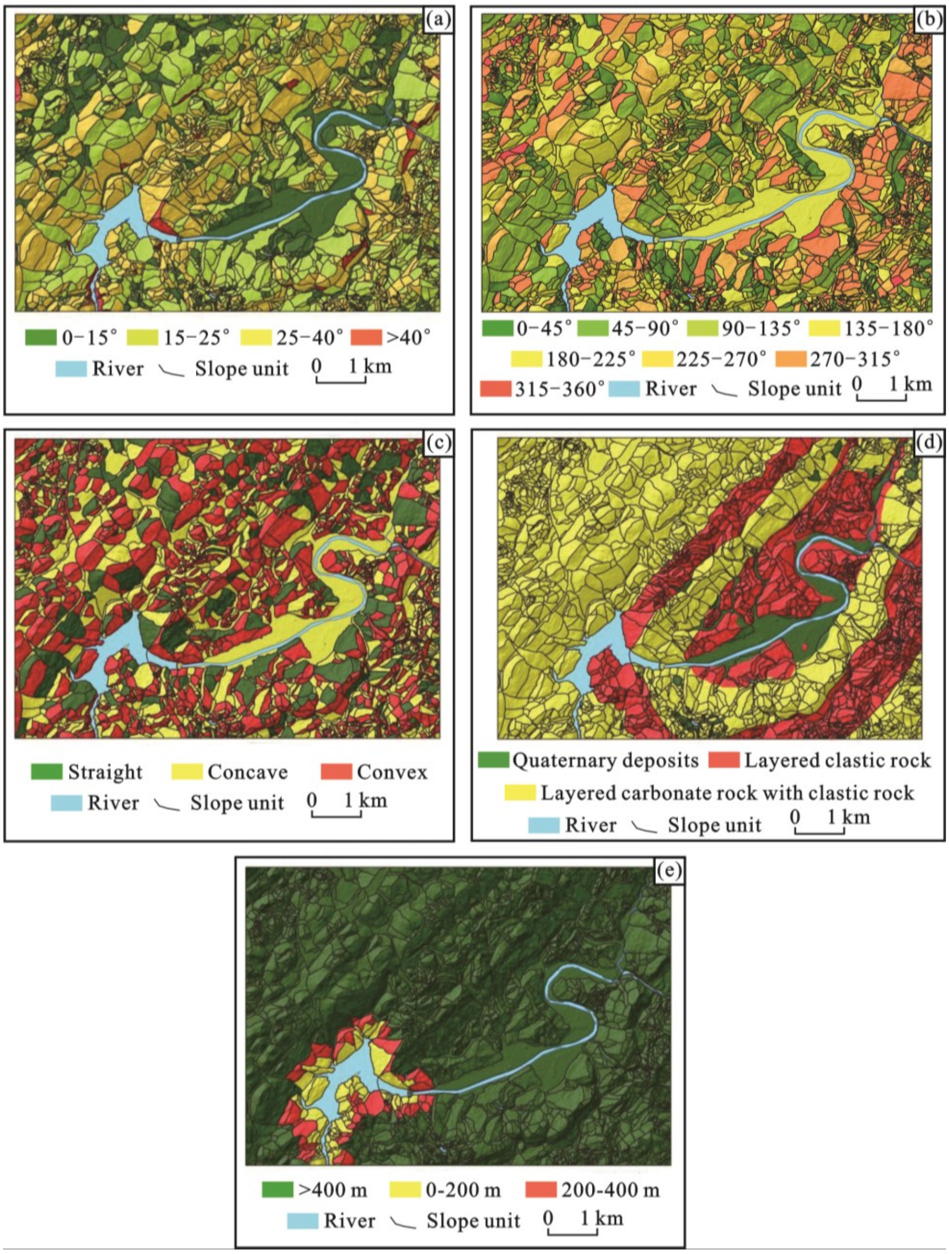

Fig. 3 Influencing factors used in the landslide susceptibility modelling: (a) slope angle; (b) aspect; (c) profile curvature; (d) lithology; (e) distance to reservoir.

Land use and land cover

Different LUC types may control the stability of slopes, of which the mechanism can be clarified by an amount of hydrological and mechanical effects, including changing hydrological functioning of hillslopes, affecting rainfall partitioning, infiltration characteristics, and runoff production, and even the shear strength of the soil (García-Ruiz et al., 2010).Meanwhile, different from several environmental factors such as geological structure and lithology, the LUC can be affected by major modifications seasonally or over a period of decades because it can be natural or induced and controlled by human actions (Reichenbach et al., 2014). Hence, for a region where the LUC types can change obviously over a relatively short period, the correlation between LUC type and landslides should be defined to assess the effect of LUC on the occurrence of landslides. For the LUC maps the evolution over time must be extracted through the comparison from at least two different time periods (Pisano et al., 2017). In this study, a time interval covering 21 years (1992-2013) was considered, which were divided into two ranges: 1992-2002 and 2002-2013. It should be noted that the maps before 1992 was not provided because of the availability of the RS images needed for the mapping procedure and the undeveloped urbanization at that time.

4. Results

4.1 Land use and land cover maps

In the process of classification, although various LUC types were identified from the RS images, some of the types were later combined for statistical analysis. For example, the lands for urban buildings, roads and mines were all combined and defined as the human engineering activities land (HEAL). Both of the grassland and arable land (GAL) are the shallow surface of the ground covered by certain vegetation, so they were considered as the same LUC type. The area covered by large amounts of tress was considered as forest land. If an area did not belong to any type of the above, which meant few plants or trees could were seen on it, it was defined as barren land. Hence, the final LUC map (Fig. 4 (a), (b) and (c)) of the study area was classified into four classes: (i) human engineering activities land; (ii) forest land; (iii) grassland and arable land; (iv) barren land. The data were then integrated in an ArcGIS environment where 2870 slope units have been delineated according to the method in 3.4 section. Finally, the characteristics of spatial distribution of different LUC types were indicated based on slope units (Fig. 4 (d), (e) and (f)). The classification accuracies of different years were evaluated by confusion matrix showed in the Table 2 and some evaluation indices were used such as producer’s accuracy (PA) and user’s accuracy (UA). Overall, all of the classification results are good with the overall accuracies (OA) approximately 90% or more than 90%. In addition, for a single LUC type, most of the PAs and UAs are larger than 80%, indicating the type was identified successfully, especially the results of 1992, which has the accuracies of larger than 90% for nearly all of the evaluation indices. Such results can provide a solid base for landslide susceptibility assessment.

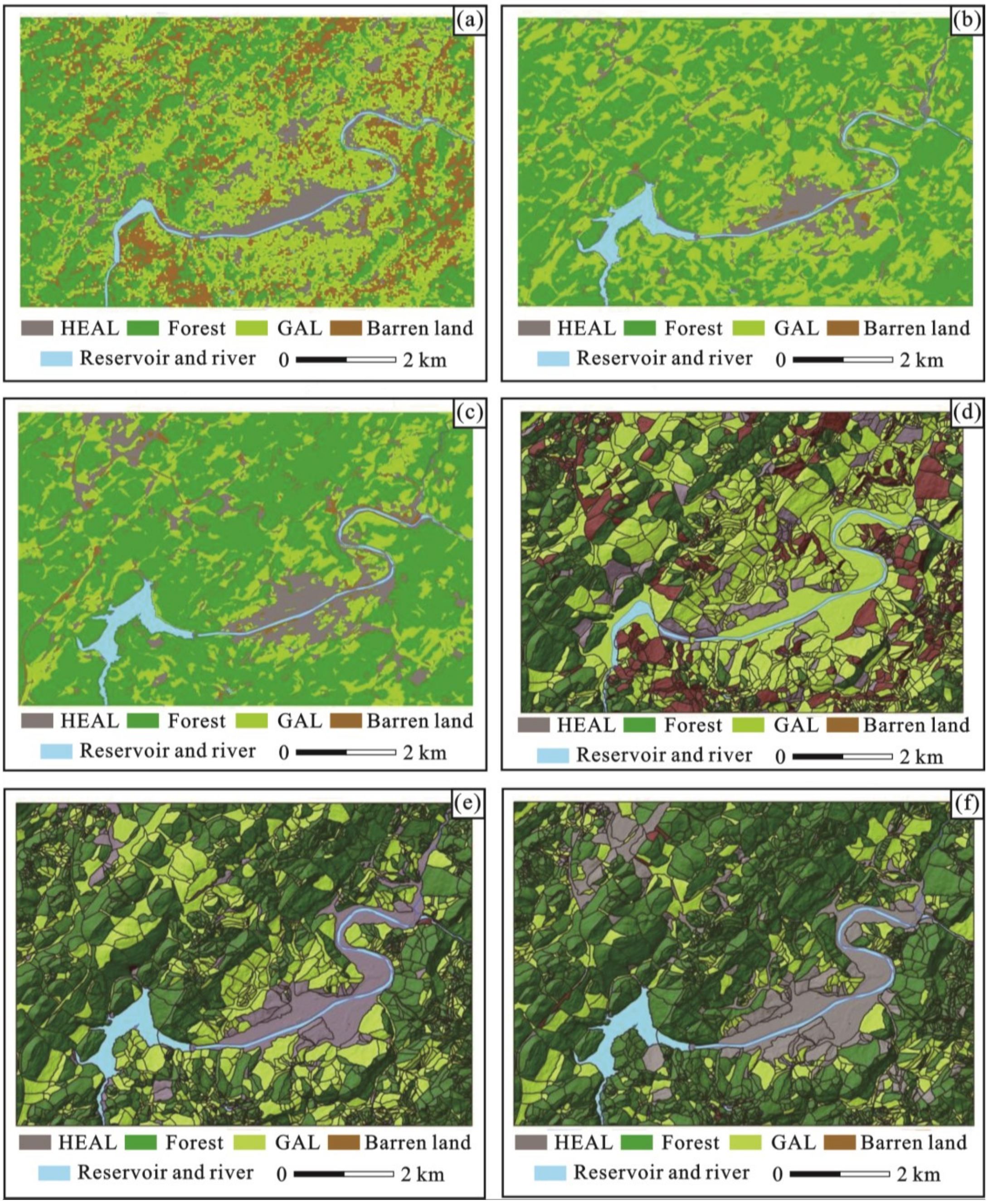

Fig. 4 (a) The LUC map of 1992; (b) The LUC map of 2002; (c) The LUC map of 2013; (d) The LUC map of 1992 based on SU; (e) The LUC map of 2002 based on SU; (f) The LUC map of 2013 based on SU.

Table 2 The classification accuracies of LUC maps for different years

Year	LUC	PA/%	UA/%	OA/%	Kappa/%
1992	HEAL	98.4	99.5	95.6	93.9
	Forest land	95.8	97.2		
	GAL	91.5	85.2		
	Barren land	94.5	97.5		
2002	HEAL	87.8	90	92.3	88.8
	Forest land	88.1	94.9		
	GAL	100	96.4		
	Barren land	83.3	62.5		
2013	HEAL	87.5	87.5	89.3	83.4
	Forest land	100	100		
	GAL	89.2	97.1		
	Barren land	91.7	73.3		

As seen in Fig. 5, from 1992 to 2013, the area of barren land has decreased obviously, mainly because the urbanization process has been continuing, leading to most of barren land was used for other purposes, such as human buildings, roads and so on. Similarly, the change of the grassland and arable land also shows the characteristic of rapid reduction. Contrary to this, the areas of the category of (i) and (ii) increased in this period, especially the forest land, with the percentage among the total area increasing from 34% in 1992 to 68.3% in 2013. Even though most studies have revealed that regional forest degradation was more likely to occur in the past decades (Karsli et al., 2009; García-Ruiz et al., 2010; Galve et al., 2015), obviously, it was not the case in our paper. In fact, some studies still support such results like ours, despite their driving forces to cause the increase of forest land are different, such as depopulation and land abandonment (Beguería, 2006), conscious landscape management (Pisano et al., 2017) and so on. In this work, the increase of forest land is mainly beneficial from two points: (i) the phenomenon of deforestation before 1992 was serious, causing a large number of natural forests disappeared. With the enhancement of awareness of environmental protection in the area, especially after the year of 2000, the environment problems have gradual been the focused issue by the decision-makers of China. National policy of "returning farmland to forest" performed since 1999 has produced a very positive results. (ii) The development of tourism industry, which calls for a better ecological environment.

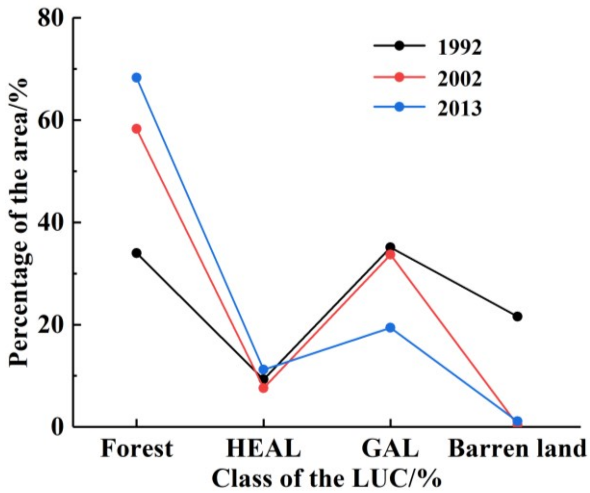

Fig. 5 The change of area of different land use and land cover types.

4.2 Landslide inventory

The inventory (Fig. 6) revealed 53 landslides in the area, of which 1 occurred in the period 1992-2002, and 10 occurred during 2002 to 2013. The total area of these landslides is 201.6×10^4 m^2, with a volume of approximately 1000×10^4 m^3. The depths of landslides in the area rang from 1 m to 15 m, among which more than 30 landslides have the depth of less than 5 m, and only 5 landslides have the depth of larger than 10 m. Hence, shallow landslides are the most important part of landslides in the area. According to the type of movement, material (Cruden and Varnes 1996) and estimated depth, most of the them are shallow earth slides, and composite soil slide–debris flows. The deformation of many landslides are characterized by cracks (Fig. 7), including tension and bulging cracks on the ground, and deformation cracks on the buildings. For some landslides in the urban area, strong slope cutting cause the small-scale sliding on the toe of them. For example, the Huanghexiang landslide (HHXL), located 500 m on the northwest side of the Qingshui River, is a shallow earth slide, which develops on the slide-prone strata of the Badong Formation (Deng et al., 2017). Under the combined effects of strata and slope cutting, HHXL was induced with many cracks observed, causing serious threat to residents.

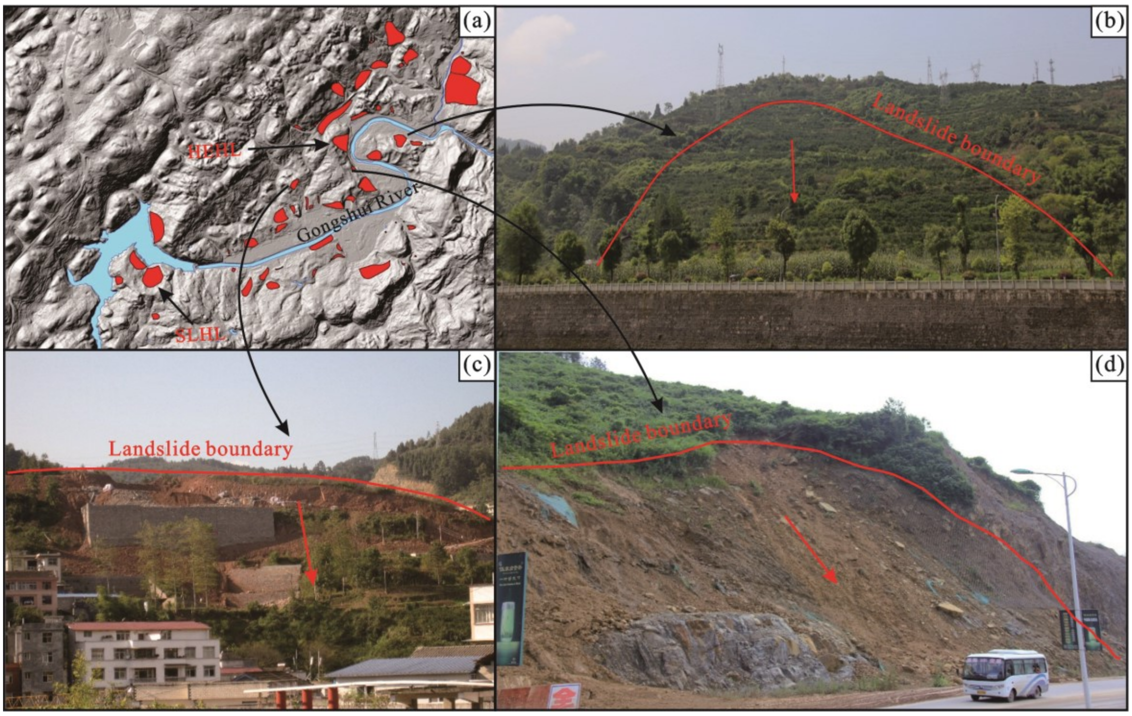

Fig. 6 The spatial locations of the landslides and the photos of different types of landslides in the study area: (a)The spatial locations of the landslides. (b)The photo of the rock slide. (c) The photo of the composite soil slide–debris flows. (d) The photo of the shallow earth slide.

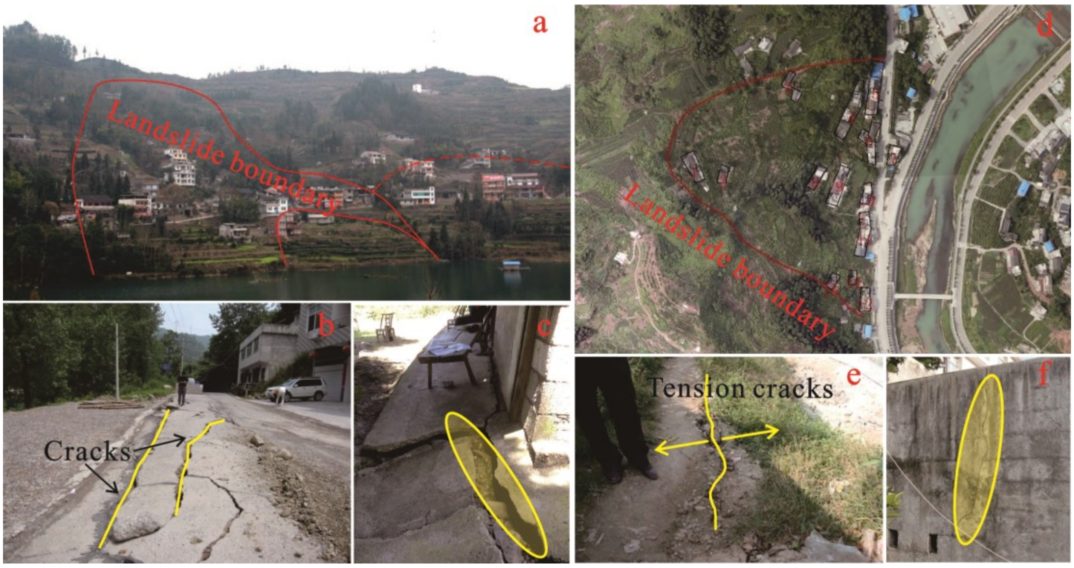

Fig. 7 The deformation of the landslides in the study area: (a) The topography of SLHL (see Fig. 6 (a) for location). (b)The cracks on the road of SLHL. (c) The uplift of the ground of SLHL. (d) The topography of HEHL (see Fig. 6 (a) for location). (e) The tension cranks of the ground on HEHL. (f) The cracks of the building of HEHL.

4.3 Landslide susceptibility zonation

Landslide susceptibility maps obtained by logistic regression model are showed in Fig. 8 (a), (c) and (e). Meanwhile, the weight of evidence model (Regmi et al., 2014; Razavizadeh et al., 2017) was utilized as the comparison model (Fig. 8 (b),

(d) and (f)). The ROC curves were applied to show the success accuracies of different models qualitatively, by plotting the cumulative percentage of observed landslide occurrence against the cumulative percentage from very high to low susceptibility with decreasing *LSI* values. As shown in the Fig. 9 and Table 3, in all six cases, all of the AUC values are larger than 80% (except the result of 2002 by weight of evidence model), showing good accuracies of the landslide susceptibility assessment. Through comparing the results of different models in the same year, we can see that the logistic regression model is better than weight of evidence model in this work. Especially, the change of ROC curves, sensitivity and specificity values of weight of evidence model in different periods are more obvious. For instance, the sensitivity values are 83.0%, 70.8% and 79.9%, respectively, while that of logistic regression model are 74.6%, 75.0% and 78.4%, respectively, indicating that the performance of logistic regression model is more stable than that of weight of evidence model.

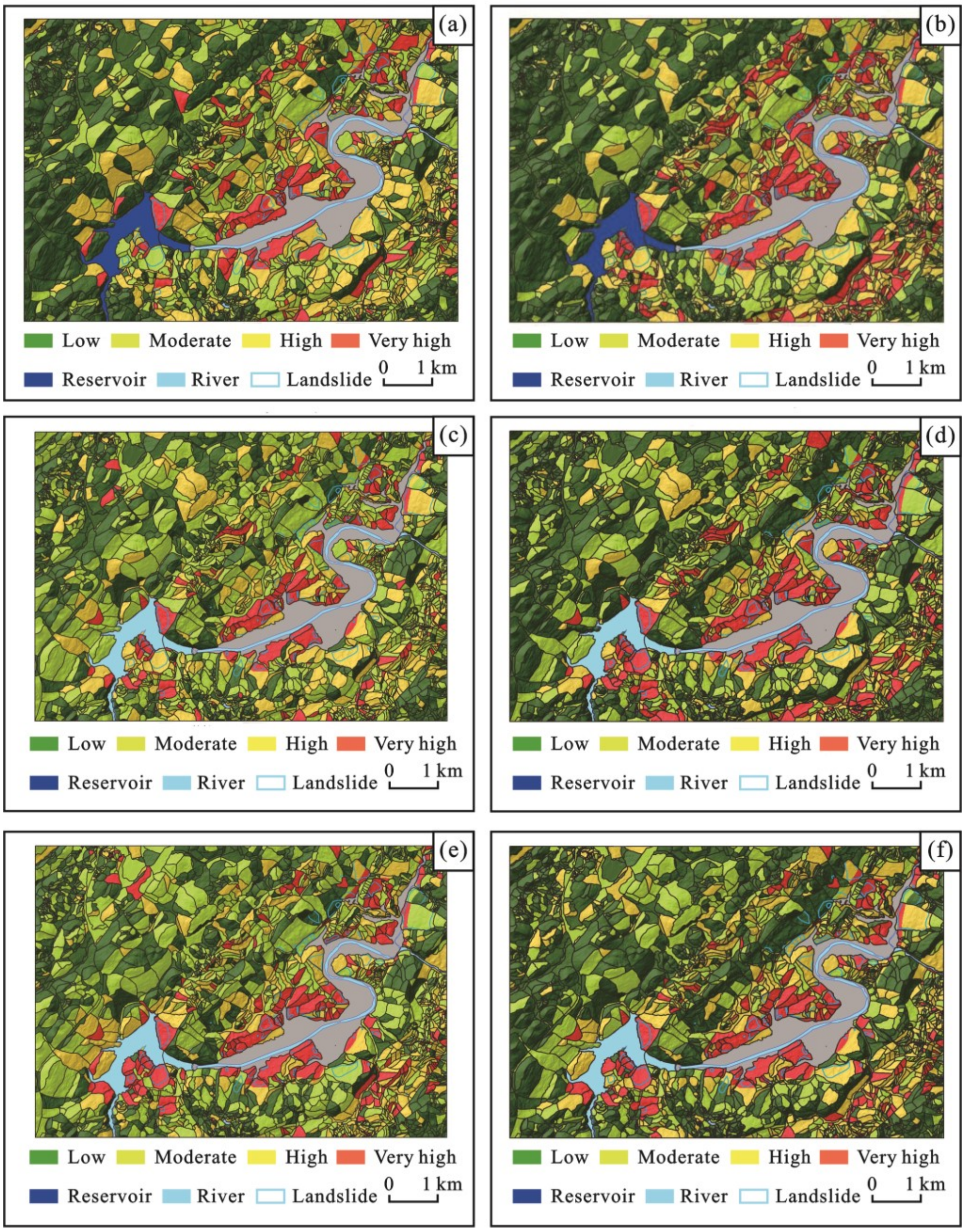

Fig. 8 The results of landslide susceptibility zonation: (a) LRM for 1992; (b) WEM for 1992; (c) LRM for 2002; (d) WEM for 2002; (e) LRM for 2013; (f) WEM for 2013.

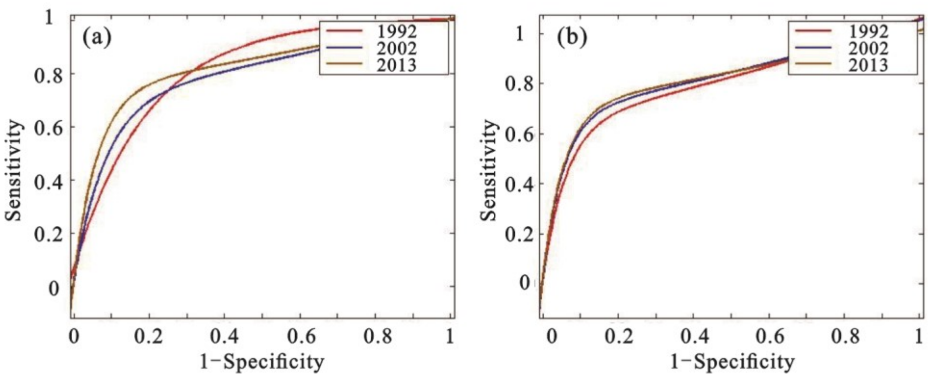

Fig. 9 The ROC curves of (a) WEM, and (b) LRM

Table 3 The accuracies of different models

Model	Year	True positive rate/%	True negative rate/%	False positive rate/%	False negative rate/%	Sensitivity /%	Specificity /%	AUC /%
Weight of evidence model	1992	1.4	66.2	32.1	0.3	83.0	67.3	81.3
	2002	1.2	76.7	21.6	0.5	70.8	78.0	78.8
	2013	1.7	73.9	24.0	0.4	79.9	75.5	82.0
Logistic regression model	1992	1.2	74.1	24.3	0.4	74.6	75.3	81.8
	2002	1.3	75.9	22.4	0.4	75.0	77.2	84.0
	2013	1.6	72.8	25.1	0.5	78.5	74.7	81.8

4.4 Evolutions of LUC and landslide susceptibility

After the preparation of mappings, the LUC and landslide susceptibility of the same locations in different periods were placed together to compare so that it is possible to clarify the evolutions of LUC and LS with a time interval covering 21 years. It should be noted that logistic regression model had been clarified to have a better performance for landslide susceptibility in this study, so the subsequent analysis was carried out in the framework of this model.

As seen in Fig. 10, in the period of 1992 – 2002, the main trend of LUCC is that the arable land transfer into forest land and the barren land transfer into arable land and forest land, especially the area of barren land decreased, from the percentage of 19.8% in 1992 to 0.2% in 2002. In contrast, the forest land increased by the percentage of 33.6%. Except the reasons stated in the 5.1 section, the data quality should also be considered: the low-resolution images of Landsat4-5TM lead to bad classification between barren land and grassland covered by sparse vegetation. Contrary to these two types of LUC, the human engineering activities land did not change obviously in the area and amount of units. This is mainly because the urbanization process during this period concentrated on the plain areas on the banks of the valley, which always belonged to one slope unit with large area due to the flat terrain. In the environmental conditions mentioned above, compared with 1992, the landslide susceptibility of 1227 units in the study area has changed in 2002 (Fig. 11), among which the landslide susceptibility of 632 units increased and that of 595 units decreased, accounting for 22.0% and 20.7%, respectively, of the amount of total slope units. Further, If the magnitude of the landslide susceptibility changes are subdivided into five classes: obvious increase (LS has increased by at least two levels, e.g., from low to high), increase, constant, decrease and obvious decrease (LS has decreased by at least two levels), it can be seen that similar with the overall change of landslide susceptibility, the amount of the units of obvious increase is also larger than that of obvious decrease. Such characteristics of LS change indicate that the LUCC from 1992-2002 made Zhushan Town a more landslide-prone area. Then, the LUCC of the units with obvious increase LS was analyzed. The LUCC under this condition can be summarized into three cases: (i) constant, (ii) human engineering activities land transferred from other types of LUC, and (iii) grassland and arable land transferred from other types of LUC. The amounts of the units of these three cases are 24, 36 and 40, respectively, which reveals that there are two important types of LUC for increasing LS in this period: increase of the human engineering activities land, and the transformation from forest land to grassland and arable land. Moreover, it is worth mentioning that in these units with obvious increase LS, none unit transfers from the human engineering activities land to other types, indicating that the impact of human engineering activities on the LUC is generally decisive so that the landslide susceptibility is hardly to change due to the internal influence to the geological conditions.

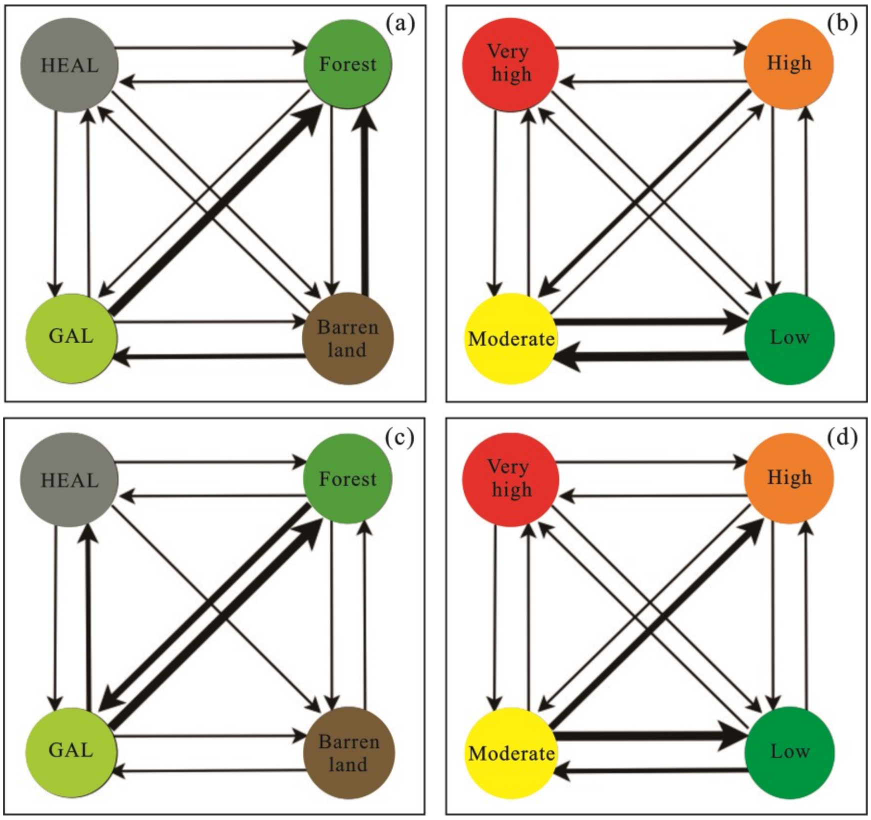

Fig. 10 (a) The transformation of LUC from 1992 to 2002; (b)The transformation of LS from 1992 to 2002; (c)The transformation of LUC from 2002 to 2013; (d)The transformation of LS from 2002 to 2013.

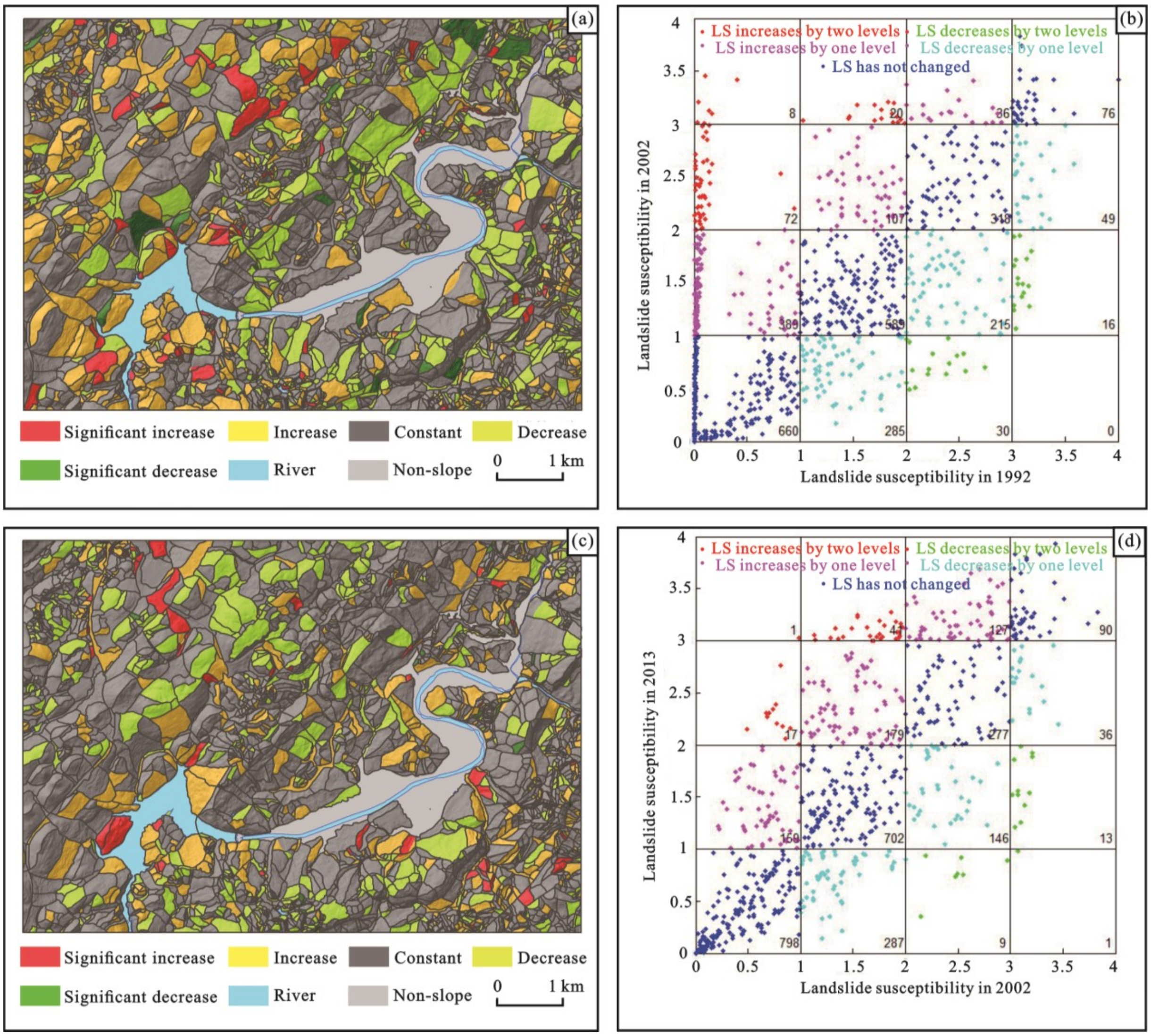

Fig. 11 (a) The change of the landslide susceptibility of each slope unit between 1992 and 2002; (b) The scatter plot showing the change of the landslide susceptibility between 1992 and 2002; (c) The change of the landslide susceptibility of each slope unit between 2002 and 2013; (d) The scatter plot showing the change of the landslide susceptibility between 2002 and 2013.

In the period of 2002 – 2013, the trend of LUCC mainly includes two aspects (Fig. 10): the first is the slightly increase of the human engineering activities land, mainly from the transformation of the grassland and arable land. Different from the previous period, the human engineering activities during this period were no longer confined to the plain areas on the banks of the valley, but carried out on the other areas, such as the northwestern part of the county. Similar situation also happened in the southeast of the county. Both areas were mainly covered by the forest land and the grassland and arable land before. The second is the increase of the forest land. Interestingly, the mutual transformation of forest land and grassland and arable land also can be seen such as the northeast of the region. This indicates that orderly and reasonable land use planning was gradually developed in this region. In other words, the focused point by the residents is not the increase of the area of the forest land anymore, but the accurate place where the forest should be planted. This is a further manifestation of the enhancement of the people's awareness of environmental protection. As a result, the land around the town in 2013 was mainly covered by forest land, not by the arable land like in the 2002. Such land use planning can effectively protect the town from the harsh environment problems (e.g., sandstorm, flood). Under such conditions of LUCC, the landslide susceptibility of 947 units has changed in 2013 (Fig. 11), among which the landslide susceptibility of 441 units increased and that of 506 units decreased, accounting for 15.4% and 17.6%, respectively, of the total units. Compared with 2002, all of these numbers are smaller, indicating that the influence of the LUCC during this period was slighter than that during 1992-2002. The units of obvious increase and obvious decrease for landslide susceptibility in 2013 were 59 and 23, respectively, also smaller than that in 2002. The LSs of most units were constant during this period. This is mainly because (i) the increase of the human engineering activities land was small, and (ii) the impact of forest land and grassland and arable land on the stability of the land was limited. Despite this, the change of landslide susceptibility influenced by the human engineering activities land is still obvious. During this period, a total of 195 units were transformed from other types of LUCC to the human engineering activities land, of which the landslide susceptibility of 161 units increased and none of units had a reduced LS. Among the total 59 units with obviously increased LS, the LUC of 46 units were transformed to the human engineering activities land, accounting for 78.0 % of the total units. Hence, the transformation to this type of LUCC played an important role in the increase of the landslide susceptibility in the region, mainly because the slope cutting in the engineering activities influenced internal geological conditions and necessary measures were not implemented due to the lack of professional knowledge.

4.5 Typical landslide events influenced by LUCC

In the period during 2002~2013, 9 landslide events occurred in the study area, among which 2 are located at the bank of the SLHR, mainly triggered by the reservoir water level. Hence, the remaining landslides were taken as the examples to explore the impact of the engineering activities on land. A 25 m buffer of each landslide was established and then the change of the engineering activities in the buffer was counted. Except one landslide, the area of the engineering activities around all landslides have expanded since 2002. Overall, the average range of engineering activities around the landslides have increased by nearly 20%, and the change mainly focused on the toe of the landslides, indicating that the under cutting of slope is common in the region.

4.5.1 The Qili Bridge Landslide (QLQL)

The QLQL (Fig. 12) located at Qili Bridge village of the Zhushan County, on the right side of the No. 209 national road.

The slope where the landslide developed had an elevation ranging from 520 m to 762 m above the sea level (ASL) and a gulley with a strike direction of 340° existed in the toe of the slope. The QLQL developed at the lower part of the slope, with an area of 9000 m^2 and a volume of 0.27×10^4 m^3. The landslide is a semicircular-shape in plane and a straight line in profile. The landslide materials mainly composed of cataclastic marl rock of Triassic and Quaternary deposits including silty clay and rubble soil.

In 2007, at the lower part of the slope, where the elevation was approximately 520 m ASL, a platform began to be constructed, and then 6 brick-and-concrete buildings with 3~4 storeys were built on the platform without any protection measures. The slope was a consequent bedding rock slope with a natural dip angle more than 30°. The steep free surface with a height of about 3 m was caused by the slope excavation. Combined with the rather cataclastic materials of the QLQL with many fissures, the rainfall infiltrated into the sliding body rapidly, making the strength of the materials gradually reduced. In July 2011, the continuous heavy rain induced the landslide. The back walls of the buildings were destroyed by the rock mass, causing some injuries and severe economic losses. As seen in Fig. 12, before the construction of the buildings, the natural slope was mainly covered by the forest land, grassland and arable land. However, the subsequent engineering activities disrupted the original geological conditions, causing the instability of the slope. Even nowadays, some sliding materials still remain on the slope, being a big potential danger for the residents.

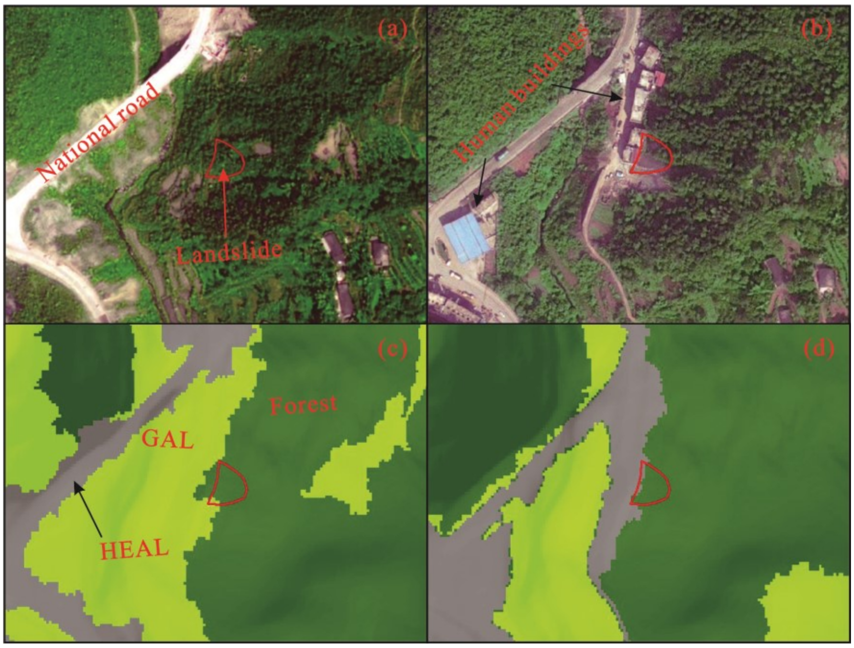

Fig. 12 The LUCC around the QLQL: (a) The RS image of QLQL in 2002（obtained from Superview-1 RS data）; (b) The RS image of QLQL in 2013 (obtained from DJI drone); (c) The LUC type of QLQL in 2002; (d) The LUC type of QLQL in 2013.

4.5.2 The Liangshuigou Landslide (LSGL)

The LSGL (Fig. 13) located at Lianhuaba village, on the left bank of the Gongshui River. The natural slope had a dip angle ranging from 25°~35° with a slope aspect of 55°. The LSGL developed at the lower part of the slope, with an area of 6300 m^2 and a volume of 0.1×10^4 m^3. The landslide is an irregular-shape in plane and step-like in profile. The landslide materials mainly composed of the Quaternary deposits including silty clay and rubble soil. The bedrock was mainly argillaceous siltstone of Badong Formation in Triassic with developed joints and fissures, which cut the rock mass into blocks.

Before 2010, the slope was mainly covered by citrus trees and crops (arable land). However, with the progress of the urbanization, many human engineering activities were performed in the nearby area, including the constructions of the building and the road. The slope cutting at the toe of the slope caused a free surface with a height of about 10 m. On June 2012, the landslide was triggered by the heavy rainfall event.

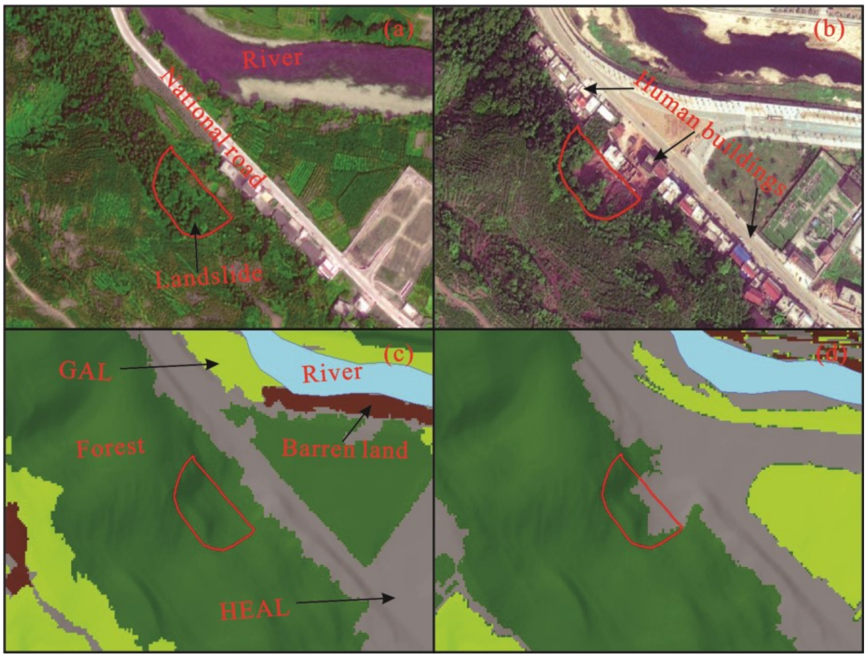

Fig. 13 The LUCC around the LSGL: (a) The RS image of LSGL in 2002（obtained from Superview-1 RS data）; (b) The RS image of LSGL in 2013 (obtained from DJI drone); (c) The LUC type of LSGL in 2002; (d) The LUC type of LSGL in 2013.

5. Discussion

Although the results highlight the significance of LUCC in the susceptibility assessment of shallow landslides, it is obvious that LUCC is not the only factor that can influence the landslide occurrence in the region. In fact, in most cases, the impact of LUC on landslides is about the internal geological conditions, such as terrain features, drainage conditions, even stress field distribution. Such impacts can worsen/improve the stability of natural slopes to increase/decrease the landslide areal frequency in these zones (Schmaltz et al., 2017; Galve et al., 2015). For instance, a case study in the Spanish Pyrenees by Beguería (2006) has verified that due to the water redistribution in the slopes after prolonged rainfall periods, the former arable fields on the valley slopes still facilitated landsliding, even after land abandonment and revegetation by shrubs or trees. However, it should be noted that the shallow landslides are directly triggered by the LUC, except some landslides induced by slope cutting effect. The statistical results of the temporal distribution of landslides in this study area also support this assumption: the positive correlation between the number of landslides and monthly average rainfall (statistical result of daily rainfall data between 1992~2013) is rather strong. The amount of landslides occurring in June and July are 18 and 12, respectively, accounting for 56.6% of the total landslides, whereas only 10 landslides did not occur in the rainy season (May ~ September), accounting for 18.9% of the total landslides. Based on this, from the perspective of the period with a 21-year interval, the change of the landslide susceptibility at regional scale is associated with rainfall conditions. As seen in Fig. 14, the overall annual rainfall between 1992 and 2013 first increases (1992~1998) and then decreases (1999~2013), although the magnitude of the change is relatively slight. Similar patterns are also showed in the amount of heavy rainfall events of this period. It should be noted that this law is roughly the same as the change of the high susceptibility area. Thus, to be exact, it's not that the LUCC can change the susceptibility directly, but the natural slope conditions are influenced by various LUC and subsequently show different environments for the landslides development. In conclusion, most landslides in the area, especially shallow landslides, were not triggered by a single factor, but the combined results of external environmental factors. For example, during the period from 6th to 26th in June 2013, although only three days were rainy (6th, 9th and 10th), the total rainfall reached up to 149.1 mm. Two landslides (i.e., 1# and 2# landslides) were triggered by this heavy rainfall event, which occurred on 16th and 26th in this month, respectively. However, if a longer time scale is taken into account, the role that human engineering activities play also become very important, because many engineering activities including buildings and road constructions were performed on the locations of these two landslides a few years ago.

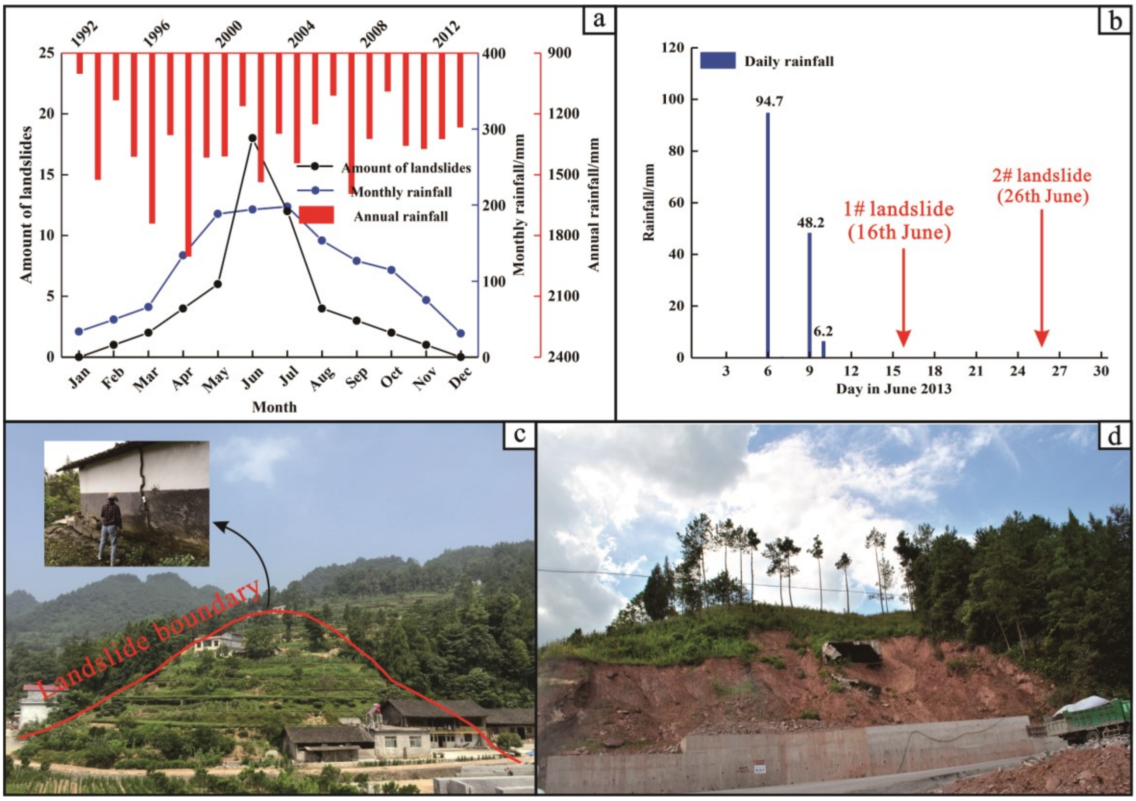

Fig. 14 The relationship between rainfall and shallow landslides in the area: (a) The curve showing monthly rainfall and temporal distribution of landslides; (b) Daily rainfall in June 2013; (c) The topography of 1# landslide; (d) The topography of 2# landslide.

In addition, the fluctuation of the reservoir water level is also a triggering factor that cannot be ignored. The SLHL is the appropriate example. Before the construction of the reservoir (1992), the slope unit where the landslide is located has moderate susceptibility, whereas it increased to very high susceptibility level in 2002 and 2013. Although the reservoir is also a kind of human engineering activities, this landslide was mainly triggered by the reservoir impoundment. Seasonal and periodic fluctuation of the reservoir water level affects the seepage conditions of inside the landslide and soften the geotechnical properties, both of which can gradually worsen the landslide stability. The field survey has captured the appearance of a large amount of cracks on the ground of SLHL after the construction of the reservoir. A nearly decade of deformation observation also indicated the slow but continuous movement of the landslide, with a velocity of approximately 1.6m/yr. In particular, the landslide movement shows an obvious intermittent characteristic: the movement accelerates in the rainy season in which period the reservoir water level generally decreases, while the movement often stops in other periods. Obviously, the landslide is undergoing the creep deformation influenced by the reservoir water level combined with rainfall. In the final analysis, however, this kind of impact was not highlighted because the reservoir area was considered as a kind of HEAL, leading that the change of the susceptibility of this slope unit was incorporated into the results of LUCC. To remedy this, specific analysis for single landslide is necessary to completely understand the triggering mechanism of the landslide, but this is not the case in our work. Hence, it can be seen that due to the limitation of the estimation model, availability of the data, and scale of the study, the impact of LUCC on landslides in this paper was partially exaggerated, especially in areas where various triggering factors (e.g., HEA, rainfall, reservoir water level, etc.) may exist at the same time.

In order to explore the impact of LUCC on landslide occurrence, it is believed that in this work the temporally and spatially differentiated information for both, landslide inventory and LUC maps are particularly important to be considered, while the other used influencing factors were considered as static factors. However, they have proven to be dynamic, with changes occurring even in few decades. Especially, in populated areas, the topographic factors (i.e., slope angle, aspect and profile curvature in this work) can be greatly altered by frequent earth surface movement processes (e.g., landslides, soil erosion, slope cutting, etc.) in a short time. Hence, a more accurate susceptibility result calls for good timeliness of initial DEM data and influencing factor maps, which in fact is seldom available, at least for an undeveloped area in the 1990s. Moreover, in landslide susceptibility evaluation, the LUC data integrate the controlling factor group and, generally, are directed by another factor input to the evaluation model. In some cases, LUC data are used as a landslide conditioning factor, which is usually scarce, generalized and not very detailed (Meneses et al., 2019). For instance, the CORINE land cover (CLC) data are widely used for landslide assessment in many regions of Europe because it is the only LUC data available (Feranec et al., 2007). A similar situation happens in the analysis of 1992 in this study. The RS data with low resolution caused the inherent uncertainties of the obtained LUC maps, which was subsequently taken into the landslide susceptibility model. Even though we have tried to reduce such uncertainties by decreasing the amount of LUC categories and using classification method of images with better accuracy, the final LS zonation results were still related with considerable uncertainties. Under this condition, it seems not to be important to compare different models to improve the accuracy of landslide susceptibility evaluation. For example, Schmaltz et al. (2017) have recommend to apply easily interpretable multi variable model or generalized additive models that allow to include potential confounders for similar studies, which is in accordance with the model used in our study.

6. Conclusion

Land use and land cover change can alter the geological conditions and affect the occurrence of the landslides. This study is to observe the evolution of LUC and detail the effects of LUC change on landslide susceptibility at a regional scale. Zhushan County in Hubei Province (China), a landslide-prone area, was taken as the study area. Through the analysis of different LUC maps with a time interval covering 21 years obtained from remote sensing images, we documented the rapid growth of the afforestation as well as intense urbanization process in this region since 1990s: the areas of forest land and human engineering activities between 1992 and 2013 increased by 34.3% and 1.9%, respectively; whereas the areas of the grassland and arable land, and the barren land decreased by 15.7% and 20.5%, respectively. Combined with other five factors (slope angle, aspect, profile curvature, lithology and distance to reservoir), the LUC was subsequently utilized for landslide susceptibility analysis in different years based on logistic regression model and slope unit. The zonation results revealed that the urban area on both sides of the river valley plain is always the area with the largest landslide susceptibility. Along with the increase of engineering construction activities, the susceptibility of many areas increases. Even some small shallow landslides were directly triggered by the transformation of LUC type (i.e., from forest land and GAL to HEAL) because original geological conditions were disrupted in this process.

Overall, the RS images with good resolution and the appropriate model for landslide susceptibility are the keys to evaluate the impact of land use and land cover change on landslide susceptibility. Although the resolution of RS images used in 1992 is not accurate enough, some evaluation indices still show a good classification accuracy of LUC maps. In addition, as a result of this study, it can be shown that human activities play an important role on the change of landslide susceptibility. Any engineering activities in the sloping area could pose landslide hazard if mitigation measures are not considered and implemented from the beginning. Consequently, the method used in the present work provides important benefits for landslide hazard mitigation efforts due to the combined use of both GIS and RS techniques. Such results not only call for a more reasonable land use planning in the urbanization process in the future, but also suggest a more systematic inclusion of LUC change in hazard assessment.

Data availability. The study relied on three sets of data: (i) the data collected by the field work, (ii) remote sensing data, and (iii) the detailed landslide investigation reports provided by China Geological Survey (Wuhan Center). The categories (i) and (2) are included in Table 1 in this paper. The detailed processing workflow for these data sets can be seen in the methodology section of this paper. Unfortunately, the regional-scale geological data is not available because this is not allowed by the rules of China Geological Survey (Wuhan Center).

Author contribution. Yin and Chen led the field work and data collection. Jin prepared the remote sensing data and processed the RS images. Chen and Guo discussed the research plan and prepared the paper together. Guo carried out the statistical analysis and prepared the figures of the paper. Chen supervised the project and Shrestha helped in the paper development and English writing. So Chen and Guo contributed equally and they were listed as co-first authors of the paper.

Competing interests. The authors declare that they have no conflict of interest.

Special issue statement. This article is part of the special issue "Natural hazards impacts on technological systems and infrastructures". It is not associated with a conference.

Acknowledgements. This work was financed by the project "Studies on spatial-temporal differences of large accumulation landslide deformation and its vulnerability model for buildings in the Three Gorges reservoir" (No. 41877525) funded by the National Natural Science Foundation of China.

References:

Abancó, C., and Hürlimann, M.: Estimate of the debris-flow entrainment using field and topographical data, Nat. Hazards, 71, 363-383, https://doi.org/10.1007/s11069-013-0930-5, 2014.

Abdul-Qadir, A. M.: Supervised classification for lithologic discrimination in Shaikh Ibrahim area, NW Iraq using Landsat images, Arab. J. Sci. Eng., 39, 437-451, https://doi.org/10.1007/s13369-013-0911-8, 2014.

Aitkenhead, M. J., Flaherty, S., and Cutler, M. E. J.: Evaluating neural networks and evidence pooling for land cover mapping, Photogramm. Eng. Remote Sens., 8, 1019-1032, https://doi.org/10.14358/PERS. 74.8.1019, 2008.

Aleotti, P., and Chowdhury, R. N.: Landslide hazard assessment: summary review and new perspectives, Bull. Eng. Geol. Environ., 58, 21-44, https://doi.org/10.1007/s100640050, 1999.

Alvioli, M., Marchesini, I, Reichenbach, P., Rossi, M., Ardizzone, F., Fiorucci, F., and Guzzetti, F.: Automatic delineation of geomorphological slope units with r. slope units v1.0 and their optimization for landslide susceptibility modeling, Geosci. Model Dev., 9, 3975-3991, https://doi.org/10.5194/gmd-9-3975-2016, 2016.

Bayramov, E., Buchroithner, M., and Bayramov, R.: Quantitative assessment of 2014–2015 land-cover changes in Azerbaijan using object-based classification of LANDSAT-8 timeseries. Model. Earth Syst. Environ., 2, 35-47, https://doi.org/10.1007/s40808-016-0088-8, 2016.

Berberoglu, S., Lloyd, C. D., Atkinson, P. M., and Curran, P. J.: The integration of spectral and textural information using neural networks for land cover mapping in the Mediterranean, Comput. Geosci., 26, 385-396, https://doi.org/10.1016/S0098-3004(99)00119-3, 2000.

Beguería, S.: Changes in land cover and shallow landslide activity: a case study in the Spanish Pyrenees, Geomorphology, 74, 196-206, https://doi.org/10.1016/j.geomorph.2005.07.018, 2006.

Blaschke, T.: Object based image analysis for remote sensing, ISPRS. J. Photogramm. Remote Sens., 65, 2-16, https://doi.org/10.1016/j.isprsjprs.2009.06.004, 2010.

Brenning, A.: Spatial prediction models for landslide hazards: review, comparison and evaluation, Nat. Hazards Earth Syst. Sci., 5, 853-862, https://doi.org/10.5194/nhess-5-853-2005, 2005.

Bruschi, V. M., Bonachea, J., Remondo, J., Gómez-Arozamena, J., Rivas, V., Barbieri, M., Capocchi, S., Soldati, M., and Cendrero, A.: Land management versus natural factors in land instability: some examples in northern Spain, Environ. Manage., 52, 398-416, https://doi.org/10.1007/s00267-013-0108-7, 2013.

Camilo, D. C., Lombardo, L., Mai, P. M., Dou, J., and Huser, R.: Handling high predictor dimensionality in slope-unit-based landslide susceptibility models through LASSO-penalized Generalized Linear Model, Environ. Model Softw., 97, 145-156, https://doi.org/10.1016/j.envsoft.2017.08.003, 2017.

Cervi, F., Berti, M., Borgatti, L., Ronchetti, F., Manenti, F., and Corsini, A: Comparing predictive capability of statistical and deterministic methods for landslide susceptibility mapping: a case study in the northern Apennines (Reggio Emilia Province, Italy), Landslides, 7, 433-444, https://doi.org/10.1007/s10346-010-0207-y, 2010.

Chen, L., van Westen, C. J., Hussin, H., Ciurean, R. L., Turkington, T., Chavarro-Rincon, D., and Shrestha, D. P.: Integrating expert opinion with modelling for quantitative multi-hazard risk assessment in the Eastern Italian Alps, Geomorphology, 273, 150-167, https://doi.org/10.1016/j.geomorph.2016.07.041, 2016.

Corsini, A., and Mulas, M.: Use of ROC curves for early warning of landslide displacement rates in response to precipitation (Piagneto landslide, Northern Apennines, Italy), Landslides, 14, 1241-1252, https://doi.org/10.1007/s10346-016-0718-8, 2017.

Cruden, D. M., and Varnes, D. J.: Landslide types and processes. In: Turner, A. K. , Schuster, R. L. (eds) Landslides, investigation and mitigation. Transportation Research Board Special Report 247.Transportation Research Board, Washington DC, pp 36-75, 1996.

Deng, Q., Fu, M., Ren, X., Liu, F., and Tang, H.: Precedent long-term gravitational deformation of large scale landslides in the Three Gorges reservoir area, China, Eng. Geol., 221, 170-183, https://doi.org/10.1016/j.enggeo.2017.02.017, 2017.

Fell, R., Corominas, J., Bonnard, C., Cascini, L., Leroi, E., and Savage, W. Z.: Guidelines for landslide susceptibility, hazard and risk zoning for land use planning, Eng. Geol., 102, 85-98, https://doi.org/10.1016/j.enggeo.2008.03.022, 2008.

Feranec, J., Hazeu, G., Christensen, S., and Jaffrain, G.: Corine land cover change detection in Europe (case studies of the Netherlands and Slovakia), Land use policy, 24, 234-247, https://doi.org/10.1016/j.landusepol.2006.02.022, 2007.

Galve, J. P., Cevasco, A., Brandolini, P., and Soldati, M.: Assessment of shallow landslide risk mitigation measures based on land use planning through probabilistic modelling, Landslides, 12, 101-114, https://doi.org/10.1007/s10346-014-0478-9, 2015.

García-Ruiz, J. M., Beguería, S., Alatorre, L. C., and Puigdefábregas, J.: Land cover changes and shallow landsliding in the flysch sector of the Spanish Pyrenees, Geomorphology, 124, 250-259, https://doi.org/10.1016/j.geomorph.2010.03.036, 2010.

Ghestem, M., Sidle, R. C., and Stokes, A.: The influence of plant root system on subsurface flow: implications for slope stability, Bioscience, 61, 869-879, https://doi.org/10.1525/bio.2011.61.11.6, 2011.

Ghestem, M., Veylon, G., Bernard, A., Vanel, Q., and Stokes, A.: Influence of plant root system morphology and architectural traits on soil shear resistance, Plant Soil., 377, 43-61, https://doi.org/10.1007/s11104-012-1572-1, 2014.

Glade, T.: Landslide occurrence as a response to land use change : a review of evidence from New Zealand, Catena, 51, 297-314, https://doi.org/10.1016/S0341-8162(02)00170-4, 2003.

Gioia, E., Carone, T., and Marincioni, F.: Rainfall and land use empirically coupled to forecast landslides in the Esino river basin, central Italy, Nat. Hazards Earth Syst. Sci., 15, 1289-1295, https://doi.org/10.5194/nhess-15-1289-2015, 2015.

Guzzetti, F., Carrara, A., Cardinali, M., and Reichenbach, P.: Landslide hazard evaluation: a review of current techniques and their application in a multi-scale study, Central Italy, Geomorphology, 31, 181-216, https://doi.org/10.1016/S0169-555X(99)00078-1, 1999.

Guzzetti, F., Cardinali, M., Reichenbach, P., and Carrara, A.: Comparing landslide maps: a case study in the upper Tiber River Basin, central Italy, Environ. Manage., 25, 247-263, https://doi.org/10.1007/s002679910020, 2000.

Guzzetti, F., Galli, M., Reichenbach, P., Ardizzone, F., and Cardinali, M.: Landslide hazard assessment in the Collazzone area, Umbria, Central Italy, Nat. Hazards Earth Syst. Sci., 6, 115-131, https://doi.org/10.5194/nhess-6-115-2006, 2006a.

Guzzetti, F., Reichenbach, P., Ardizzone, F., Cardinali, M., and Galli, M.: Estimating the quality of landslide susceptibility models, Geomorphology, 81, 166-184, https://doi.org/10.1016/j.geomorph.2006.04.007, 2006b.

Guillard, C., and Zêzere, J.: Landslide susceptibility assessment and validation in the framework of municipal planning in

Portugal: the case of Loures Municipality, Environ. Manage., 50, 721-735, https://doi.org/10.1007/s00267-012-9921-7, 2012.

Harris, C., Davies, M. C. R., and Etzelmüller, B.: The assessment of potential geotechnical hazards associated with mountain permafrost in a warming global climate, Permafrost Periglac., 12, 145-156, https://doi.org/10.1002/ppp.376, 2001.

Huang, F., Yin, K., Huang, J., Gui, L., and Wang, P.: Landslide susceptibility mapping based on self-organizing-map network and extreme learning machine, Eng. Geol., 223, 11-22, https://doi.org/10.1016/j.enggeo.2017.04.013, 2017.

Huang, F., Chen, L., Yin, K., Huang, J., and Gui, L.: Object-oriented change detection and damage assessment using high-resolution remote sensing images, Tangjiao Landslide, Three Gorges Reservoir, China. Environ. Earth Sci., 77, 183-201, https://doi.org/10.1007/s12665-018-7334-5, 2018.

Iqbal, J., Dai, F., Hong, M., Tu, X., and Xie, Q.: Failure Mechanism and Stability Analysis of an Active Landslide in the Xiangjiaba Reservoir Area, Southwest China, J. Earth Sci., 29, 646-661, https://doi.org/10.1007/s12583-017-0753-5, 2018.

Karsli, F., Atasoy, M.,. Yalcin, A., Reis, S., Demir, O., and Gokceoglu, C: Effects of land-use changes on landslides in a landslide-prone area (Ardesen, Rize, NE Turkey), Environ. Monit. Assess., 156, 241-255, https://doi.org/10.1007/s10661-008-0481-5, 2009.

Kayastha, P.: Landslide susceptibility mapping and factor effect analysis using frequency ratio in a catchment scale: a case study from Garuwa sub-basin, East Nepal, Arab, J. Geosci., 8, 8601-8613, https://doi.org/10.1007/s12517-015-1831-6, 2015.

Lee, S., Ryu, J. H., Won, J. S., and Park, H. J.: Determination and application of the weights for landslide susceptibility mapping using an artificial neural network, Eng. Geol., 71, 289-302, https://doi.org/10.1016/S0013-7952(03)00142-X, 2004.

Lee, S.: Application of logistic regression model and its validation for landslide susceptibility mapping using GIS and remote sensing data, Int. J. Remote Sens., 26, 1477-1491, https://doi.org/10.1080/01431160412331331012, 2005.

Li, Z., Feng, Y., Dessay, N., Delaitre, E., Gurgel, H., and Gong, P.: Continuous monitoring of the spatio-temporal patterns of surface water in response to land use and land cover types in a Mediterranean lagoon complex, Remote Sens., 11, 1425-1443, https://doi.org/10.3390/rs11121425, 2019.

Lopez-Saez, J., Corona, C., Eckert, N., Stoffel, M., Bourrier, F., and Berger, F.: Impacts of land-use and land-cover changes on rockfall propagation: Insights from the Grenoble conurbation, Sci. Total Environ., 547, 345-355, https://doi.org/10.1016/j.scitotenv.2015.12.148, 2016.

Lombardo, L., and Mai, P. M.: Presenting logistic regression-based landslide susceptibility results, Eng. Geol., 244, 14-24, https://doi.org/10.1016/j.enggeo.2018.07.019, 2018.

Mao, Z., Yang, M., Bourrier, F., and Fourcaud, T.: Evaluation of root reinforcement models using numerical modelling approaches, Plant Soil, 382, 249-270, https://doi.org/10.1007/s11104-014-2116-7, 2014.

Mashimbye, Z. E., Clercq, W. P., and Niekerk, A. V.: An evaluation of digital elevation models (DEMs) for delineating land components, Geoderma, 213, 312-319, https://doi.org/10.1016/j.geoderma.2013.08.023, 2014.

Melchiorre, C., Matteucci, M., Azzoni, A., and Zanchi, A.: Artificial neural networks and cluster analysis in landslide susceptibility zonation, Geomorphology, 94, 379-400, https://doi.org/10.1016/j.geomorph.2006.10.035, 2008.

Meneses, B. M., Pereira, S., and Reis, E.: Effects of different land use and land cover data on the landslide susceptibility zonation of road networks, Nat. Hazards Earth Syst. Sci., 19, 471-487, https://doi.org/10.5194/nhess-19-471-2019, 2019.

Mohammady, M., Pourghasemi, H. R., and Pradhan, B.: Landslide susceptibility mapping at Golestan Province, Iran: A comparison between frequency ratio, Dempster–Shafer, and weights-of-evidence models, J. Asian Earth Sci., 61, 221-236, https://doi.org/10.1016/j.jseaes.2012.10.005, 2012.

Nandi, A., and Shakoor, A.: A GIS-based landslide susceptibility evaluation using bivariate and multivariate statistical analyses, Eng. Geol., 110, 11-20, https://doi.org/10.1016/j.enggeo.2009.10.001, 2009.

Ozdemir, A., and Altural, T.: A comparative study of frequency ratio, weights of evidence and logistic regression methods for landslide susceptibility mapping: Sultan Mountains, SW Turkey, J. Asian Earth Sci., 64, 180-197, https://doi.org/10.1016/j.jseaes.2012.12.014, 2013.

Piacentini, D., Troiani , F., Soldati, M., Notarnicola, C., Savelli, D., Schneiderbauer, S., and Strada, C.: Statistical analysis for assessing shallow-landslide susceptibility in South Tyrol (south-eastern Alps, Italy), Geomorphology, 151-152, 196-206, https://doi.org/10.1016/j.geomorph.2012.02.003, 2012.

Pinyol, N. M., Alonso, E. E., Corominas, J., and Moya, J.: Canelles landslide: modeling rapid drawdown and fast potential sliding, Landslides, 9, 33-51, https://doi.org/10.1007/s10346-011-0246-x, 2012.

Promper, C., Gassner, C. H., and Glade, T.: Spatiotemporal patterns of landslide exposure – a step within future landslide risk analysis on a regional scale applied in Waidhofen/YBBs Austria, Int. J. Disast. Risk Re., 12, 25-33, https://doi.org/10.1016/j.ijdrr.2014.11.003, 2015.

Pisano, L., Zumpano, V., Malek, Ž., Rosskopf, C. M., and Parise, M.: Variations in the susceptibility to landslides, as a consequence of landcover changes: A look to the past, and another towards the future, Sci. Total Environ., 601-602, 1147-1159, https://doi.org/10.1016/j.scitotenv.2017.05.231, 2017.

Pourghasemi. H. R., and Rossi, M.: Landslide susceptibility modeling in a landslide prone area in Mazandarn Province, north of Iran: a comparison between GLM, GAM, MARS, and M-AHP methods, Theor. Appl. Climatol., 130, 609-633, https://doi.org/10.1007/s00704-016-1919-2, 2017.

Razavizadeh, S., Solaimani, K., Massironi, M., and Kavian, A.: Mapping landslide susceptibility with frequency ratio, statistical index, and weights of evidence models: a case study in northern Iran, Environ. Earth Sci., 76, 499-514, https://doi.org/10.1007/s12665-017-6839-7, 2017.

Regmi, A. D., Devkota, K. C., Yoshida, K., Pradhan, B., Pourghasemi, H. R., Kumamoto, T., and Akgun, A.: Application of frequency ratio, statistical index, and weights-of-evidence models and their comparison in landslide susceptibility mapping in central Nepal Himalaya, Arab. J. Geosci., 7, 725-742, https://doi.org/10.1007/s12517-012-0807-z, 2014.

Regmi, N. R., Giardino, J. R., and Vitek, J. D.: Assessing susceptibility to landslides: Using models to understand observed changes in slopes, Geomorphology, 122, 25-38, https://doi.org/10.1016/j.geomorph.2010.05.009, 2010.

Reichenbach, P., Busca, C., Mondini, A. C., and Rossi, M.: The influence of land use change on landslide susceptibility zonation: the Briga Catchment test site (Messina, Italy), Environ. Manage., 54, 1372-1384, https://doi.org/10.1007/s00267-014-0357-0, 2014.

Revellino, P., Guadagno, F. M., and Hungr, O.: Morphological methods and dynamic modelling in landslide hazard assessment of the Campania Apennine carbonate slope, Landslides, 5, 59-70, https://doi.org/10.1007/s10346-007-0103-2, 2008.

Rotigliano, E., Cappadonia, C., Conoscenti, C., Costanzo, D., and Agnesi, V.: Slope units-based flow susceptibility model: using validation tests to select controlling factors, Nat. Hazards, 61, 143-153, https://doi.org/10.1007/s11069-011-9846-0, 2012.

Scalenghe, R., and Marsan, F. A.: The anthropogenic sealing of soils in urban areas. Landscape Urban Plan., 90, 1-10, https://doi.org/10.1016/j.landurbplan.2008.10.011, 2009.

Schlögel, R., Marchesini, I., Alvioli, M., Reichenbach, P., Rossi, M., and Malet, J. P.: Optimizing landslide susceptibility zonation: Effects of DEM spatial resolution and slope unit delineation on logistic regression models, Geomorphology, 301, 10-20, https://doi.org/10.1016/j.geomorph.2017.10.018, 2018.

Schmaltz, E. M., Steger, S., and Glade, T.: The influence of forest cover on landslide occurrence explored with spatio-temporal information, Geomorphology, 290, 250-264, https://doi.org/10.1016/j.geomorph.2017.04.024, 2017.

Shrestha, D. P., Saepuloh, A., and Van Der Meer, F.: Land cover classification in the tropics, solving the problem of cloud covered areas using topographic parameters, Int. J. Appl. Earth Obs, 77, 84-93. https://doi.org/10.1016/j.jag.2018.12.010, 2019.

Tasser, E., Mader, M., and Tappeiner, U.: Basic and applied ecology effects of land use in alpine grasslands on the probability of landslides, Basic Appl. Ecol., 280, 271-280, https://doi.org/10.1078/1439-1791-00153, 2003.

Taubenböck, H., Wurm, M., Netzband, M., Zwenzner, H., Roth, A., Rahman, A., and Dech, S.: Flood risks in urbanized areas – multi-sensorial approaches using remotely sensed data for risk assessment, Nat. Hazards Earth Syst. Sci., 11, 431-444, https://doi.org/10.5194/nhess-11-431-2011, 2011.

Tian, Y., Xu, C., Ma, S., Wang, S., and Zhang, H.: Inventory and Spatial Distribution of Landslides Triggered by the 8th August 2017 MW 6.5 Jiuzhaigou Earthquake, China, J. Earth Sci., 30, 206-217, https://doi.org/10.1007/s12583-018-0869-2, 2019.

Van Den Eeckhaut, M., Reichenbach, P., Guzzetti, F., Rossi, M., and Poesen, J.: Combined landslide inventory and susceptibility assessment based on different mapping units: an example from the Flemish Ardennes, Belgium, Nat. Hazards Earth Syst. Sci., 9, 507-521, https://doi.org/10.5194/nhess-9-507-2009, 2009.

Van Westen, C. J., van Asch, T. W. J., and Soeters, R.: Landslide hazard and risk zonation—why is it still so difficult? Bull. Eng. Geol. Environ., 65, 167-184, https://doi.org/10.1007/s10064-005-0023-0, 2006.

Van Westen, C. J., Castellanos, E., and Kuriakose, S. L.: Spatial data for landslide susceptibility, hazard, and vulnerability assessment: An overview, Eng Geol., 102, 112-131, https://doi.org/10.1016/j.enggeo.2008.03.010, 2008.

Vasu, N. N., and Lee, S. R.: A hybrid feature selection algorithm integrating an extreme learning machine for landslide susceptibility modeling of Mt. Woomyeon, South Korea, Geomorphology, 263, 50-70, https://doi.org/10.1016/j.geomorph.2016.03.023, 2016.

Wang, F., Yin, K. Gui, L., and Chen, L.: Risk Analysis on Individual Reservoir Bank Landslide and Its Generated Wave, Earth Sci., 43, 899-909 (in Chinese with English abstract), https://doi.org/ 10.3799/dqkx.2018.910, 2018.

Xie, M., Esaki, T., and Zhou, G.: GIS-based probabilistic mapping of landslide hazard using a three-dimensional deterministic model, Nat. Hazards, 33, 265-282, https://doi.org/10.1023/B:NHAZ.0000037036.01850.0d, 2004.

Yalcin, A., Reis, S., Aydinoglu, A. C., and Yomralioglu, T. A.: GIS-based comparative study of frequency ratio, analytical hierarchy process, bivariate statistics and logistics regression methods for landslide susceptibility mapping in Trabzon, NE Turkey, Catena, 85, 274-287, https://doi.org/10.1016/j.catena.2011.01.014, 2011.

Ymeti, I., Van Der Werff, H., Shrestha, D. P., Jetten, V. G., Lievens, C., and Van Der Meer, F.: Using color, texture and objected-based image analysis of multi-temporal camera data to monitor soil aggregate breakdown, Sensors, 17, 1241-1261, https://doi.org/10.3390/s17061241, 2017.

Zhang, T., and Tang, H.: A Comprehensive Evaluation of Approaches for Built-Up Area Extraction from Landsat OLI Images Using Massive Samples, Sensors, 11, 2-13, https://doi.org/10.3390/rs11010002, 2019.

Zhou, C., Yin, K., Cao, Y., Ahmed, B., Li, Y., Catani, F., and Pourghasemi, H. R.: Landslide susceptibility modeling applying machine learning methods: A case study from Longju in the Three Gorges Reservoir area, China, Comput. Geosci., 112, 23-37, https://doi.org/10.1016/j.cageo.2017.11.019, 2018